AD-A070 741 SPIRE CORP BEDFORD MA F/G 13/8
BROADENED CAPABILITIES IN ELECTROSTATIC BONDING FOR SOLAR CELL --ETC(U)
MAR 79 P R YOUNGER, G A LANDIS, R G TOBIN F33615-77-C-3120
UNCLASSIFIED IR-79-10057-01 AFAPL-TR-79-2008 NL

1 OF 1
AD A070741

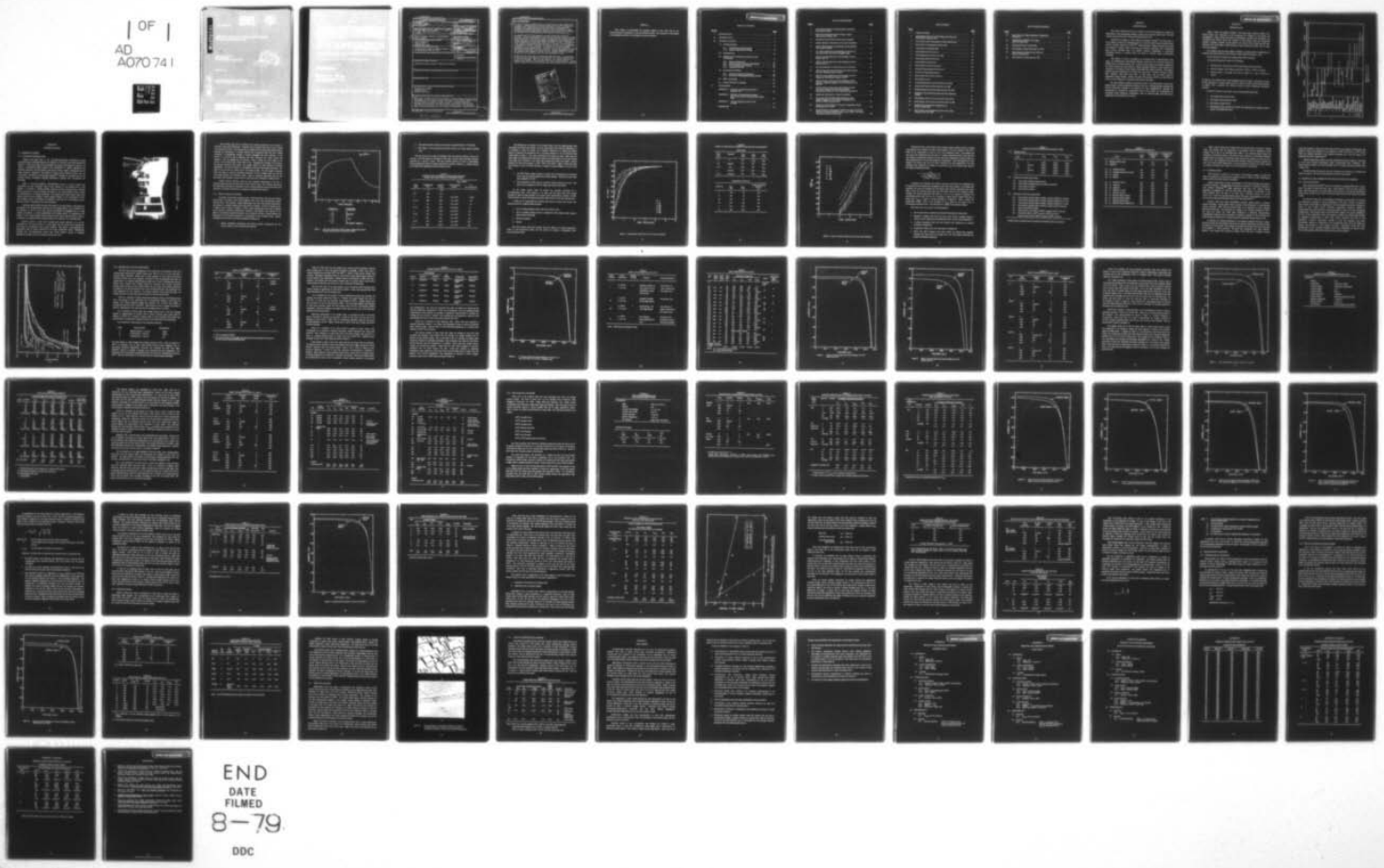

END
DATE FILMED
8-79
DDC

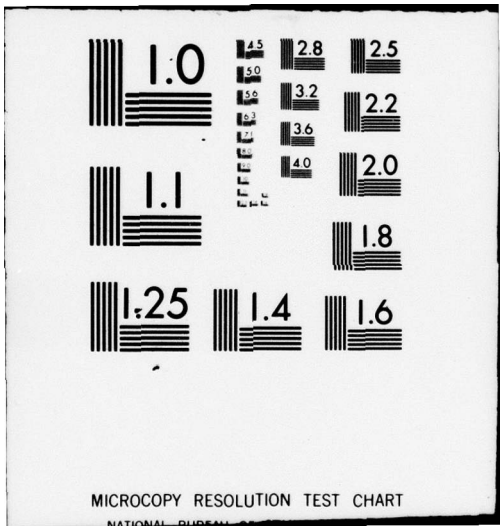
1.0
1.1
1.25
1.4
1.6
1.8
2.0
2.2
2.5
2.8
3.2
3.6
4.0
4.5
5.0
5.6
6.3
MICROCOPY RESOLUTION TEST CHART

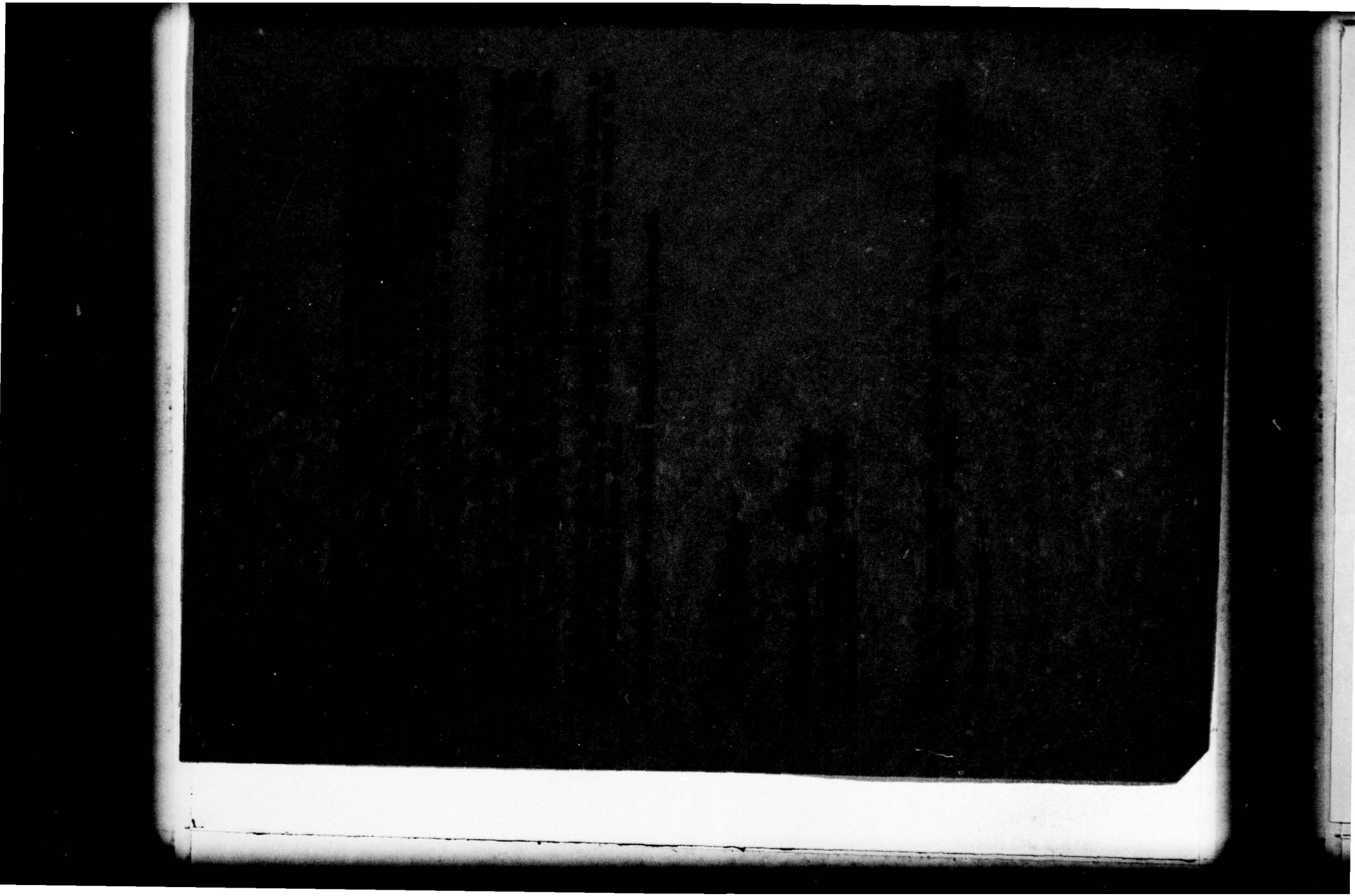

Unclassified

SECURITY CLASSIFICATION OF THIS PAGE (When Data Entered)

REPORT DOCUMENTATION PAGE

READ INSTRUCTIONS BEFORE COMPLETING FORM

1. REPORT NUMBER: AFAPL-TR-79-2008	2. GOVT ACCESSION NO.
3. RECIPIENT'S CATALOG NUMBER	
4. TITLE (and Subtitle): BROADENED CAPABILITIES IN ELECTROSTATIC BONDING FOR SOLAR CELL COVER GLASSES.	5. TYPE OF REPORT & PERIOD COVERED: Interim Technical Report. January - Dec[illegible] 1978
	6. PERFORMING ORG. REPORT NUMBER: IR-79-10057-01
7. AUTHOR(s): Peter R. Younger, Geoffrey A. Landis, and Roger G. Tobin	8. CONTRACT OR GRANT NUMBER(s): Air Force Contract F33615-77-C-3120
9. PERFORMING ORGANIZATION NAME AND ADDRESS: Spire Corporation, Patriots Park, Bedford, MA 01730	10. PROGRAM ELEMENT, PROJECT, TASK AREA & WORK UNIT NUMBERS: 3145-19-63
11. CONTROLLING OFFICE NAME AND ADDRESS: Air Force Aero Propulsion Laboratory/POE-2, Wright-Patterson AFB, OH 45433	12. REPORT DATE: Mar[illegible]79
	13. NUMBER OF PAGES: 76
14. MONITORING AGENCY NAME & ADDRESS (if different from Controlling Office)	15. SECURITY CLASS. (of this report): Unclassified
	15a. DECLASSIFICATION/DOWNGRADING SCHEDULE

16. DISTRIBUTION STATEMENT (of this Report)

Approved for public release; distribution unlimited.

17. DISTRIBUTION STATEMENT (of the abstract entered in Block 20, if different from Report)

18. SUPPLEMENTARY NOTES

19. KEY WORDS (Continue on reverse side if necessary and identify by block number)

Electrostatic Bonding
Integral Covers
Silicon Solar Cells

20. ABSTRACT (Continue on reverse side if necessary and identify by block number)

This report describes the first 12 months of a program aimed at furthering the development of electrostatic bonding techniques, so that integral glass covers can be attached to a variety of solar cell types, including those with multiple-layer antireflection (MLAR) coatings, the vertical junction cell, and texture etched cells. The electrostatic bonding facility is described. Tests of electron darkening of cover glasses are discussed. Detailed results

→ next page

DD FORM 1 JAN 73 1473 EDITION OF 1 NOV 65 IS OBSOLETE

Unclassified

SECURITY CLASSIFICATION OF THIS PAGE (When Data Entered)

393 483

Block 20 (Continued):

of efforts to apply integral covers to various groups of MLAR coated cells are given. Variations upon the program baseline cell are to be tested to determine their compatibility with the electrostatic bonding process. Variations in contact metallization tested to date are discussed. Other variations include junction depth, dimensions (both lateral and thickness), and inclusion of back surface fields and wraparound contacts.

The baseline cell for this program is an MLAR coated OCLI 2 Ω-cm n/p structure. Contact metallization is TiAg on the front and TiPdAg on the back. Postbond power is in the 62-64 mW range, although 68-70 mW has been achieved. Bonding done under controlled environment has eliminated deterioration in contact adhesion that occurs when ambient atmosphere is used. Environmental control allows more severe bonding conditions to be used, so that lines to 6 micrometers in height (twice that of previous efforts) can be accommodated at densities of up to 14 lines/cm. To compensate for possible thermal degradation during bonding, process variations, such as two temperature cycles and modified electrodes, have been introduced. Thermal degradation of some cell types has been studied in detail, but the possible effects of bonding voltage upon cell performance have not been determined to date.

Bonding to cells other than the program baseline has begun. In particular, 10 Ω-cm OCLI cells with back surface fields have also yielded postbond power in the 62-64 mW range. This cell type appears to be equally suitable for bonding as the baseline, low-resistivity cell and may perform better. Initial results obtained with vertical junction and texture etched cells are reported.

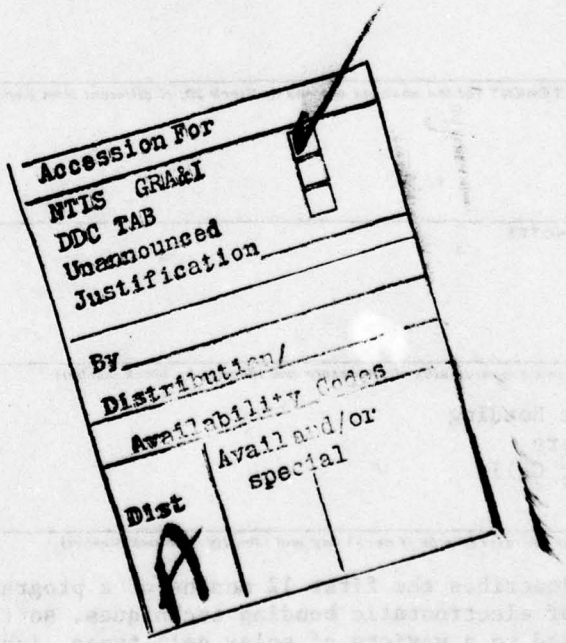

PREFACE

Spire wishes to acknowledge the extensive support of Mr. Peter Iles of the Photoelectronics Corporation of America (formerly OCLI). His cooperation in developing and supplying solar cells for this program has been invaluable.

TABLE OF CONTENTS

LIST OF ILLUSTRATIONS

LIST OF TABLES

LIST OF TABLES (Concluded)

SECTION I

INTRODUCTION

This report describes the first 12 months of a 30-month program to broaden the capabilities of the electrostatic bonding of glass covers to silicon solar cells. The work covered was performed from January through December 1978.

Electrostatic bonding, or field assisted metal-glass sealing,[1] has been shown to be an effective method for attaching covers to a variety of solar cells, as reported under AFAPL Contract F33615-74-C-2001.[2,3] Electrostatically bonded integral covers show the promise of having definite technical and economic superiority over conventional glued covers, including laser and radiation hardness, adaptability to automated processing, absence of residual stress, and ability to tolerate severe environmental conditions.

This program is aimed at bonding to the following types of high-efficiency solar cells: the multiple-layer antireflection (MLAR) coated cell, the textured surface cell (HESP), and the vertical junction cell. During the first phase of the program, bonding to the MLAR coated cell was studied in detail, including variations in grid patterns and materials, the inclusion of back surface fields (BSF) and shallow junctions. The program baseline has been established as an MLAR cell made from 1-3 ohm-cm material, without BSF. Excellent bonds have been made to these cells, with very little electrical degradation during bonding. Cycling of bonded cells between -195°C and +100°C has no effect on the mechanical or electrical performance of the bonds.

The most difficult problems encountered relate to the deformation of flat cover glasses around a raised metallization pattern on the cell. Altering bonding conditions has proved deformation bonding to be practical for most configurations. Although the temperature for forming the electrostatic bond is not critical, the temperatures for deforming around substantial metallization must be relatively high, with bond times lengthened to allow plastic flow to occur.

SECTION II

PROGRAM PLAN

Table 1 shows the program schedule. The initial phase involved studies of the MLAR coated cell. Variations in cell parameters are included in the MLAR cell investigations. These include variations in metallization material, base resistivity, cell dimensions, and junction depth, and inclusion of back surface fields and wraparound contacts. Bonding of sample vertical junction and texture-etched silicon has just been initiated, with the bonding of high-efficiency vertical junction and HESP cells to begin later in the program.

The program plan has been slightly modified to include greater consideration of bondable cells with refractory metal contacts. These studies will begin in 1979.

Panel mounting of multiple cell configurations will be developed.

Accelerated testing will consist of the following:

1. Humidity test: Thirty days at 45°C and 95 percent relative humidity.
2. Thermal cycling: Three hundred cycles from -150°C to +150°C in vacuum.
3. Thermal shock: Ten cycles from 50°C to 600°C at a rate of 100°C per minute.

A minimum of 10 bonded cells of each configuration will be tested. Preliminary in-house testing, consisting of a thermal shock test from -196°C to +100°C, will be done routinely on typical cells to identify any potential problems before fabricating deliverable hardware.

Deliverable hardware will consist of the following bonded assemblies:

1. One hundred MLAR coated cells.
2. One hundred vertical junction cells.
3. One hundred textured cells.
4. Miscellaneous cells provided by AFAPL and representative samples produced as part of developmental work.

TABLE 1
PROGRAM SCHEDULE

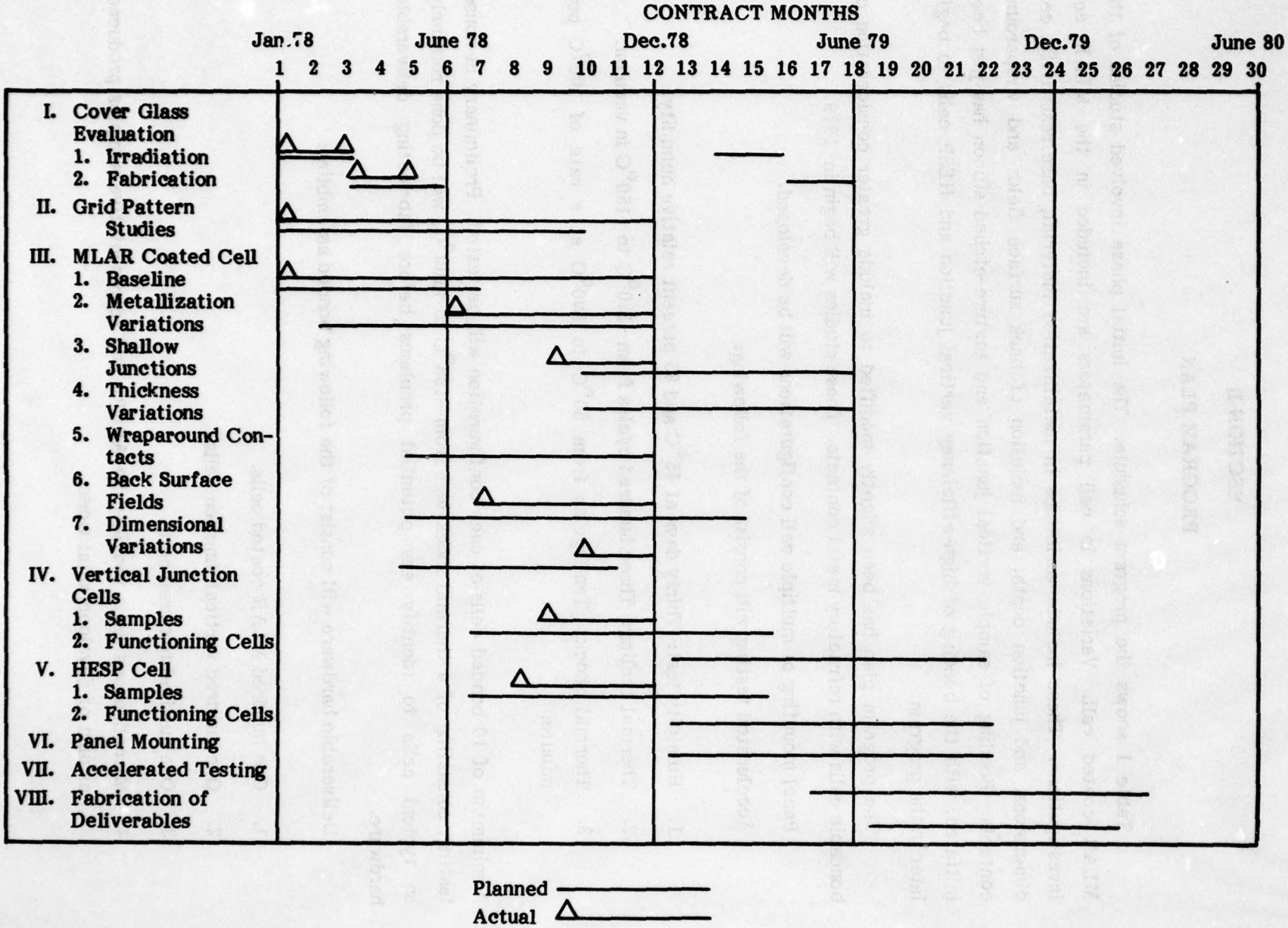

SECTION III

TECHNICAL STATUS

3.1 BONDING FACILITIES

3.1.1 Electrostatic Bonding Facility

Bonding has been done in the controlled-environment electrostatic bonder constructed under JPL/DOE Contract No. 954521 for terrestrial solar array bonding (see Figure 1). Bonds can be done in an atmosphere of nitrogen, forming gas, or helium, or in vacuum. Atmospheric control results in the elimination of contact degradation and adherence problems. For this reason, bonds can be made at higher temperatures and for longer durations, resulting in the ability to deform around contacts thicker than the 3-micrometer specified in the previous program.[3] Nitrogen is currently used as the standard bonding atmosphere, although experiments involving other atmospheres are continuing.

Under a concurrent program, microprocessor control of all the major bond parameters has been developed. This is now standard for all bonding done in this program. In addition to making possible relatively complex bonding cycles, including slowly ramped bond current, voltage, and pressure, the microprocessor control insures the reproducibility of bonding conditions. The programmable high-voltage supply also allows constant-current bonding, constant-voltage bonding, or any combination of both. Bond voltage, current, and pressure are graphed in real time on a CRT display, and the graph is copied for reference at the end of each bond.

A sample preheat facility has also been added to the bond facility. This allows the preheating of the samples before insertion into the bonding region. It was intended that the preheater be set to a level where thermal degradation is negligible, but at a high enough temperature to reduce significantly the cooling effect of transferring cold samples to the bonding region; thus the primary heater plates will not drop as much in temperature on sample insertion, allowing deformation conditions to be reached sooner.

Another method to avoid heater cooling upon sample insertion is to set the temperature of the heater plates to a value higher than the actual bond temperature, then reset the temperature after sample insertion. This results in compensating the temperature drop on sample insertion by the initial temperature offset. Experiments utilizing this "two-temperature cycle" have shown positive results in reducing degradation through cycle time reduction (see Section 3.3.2).

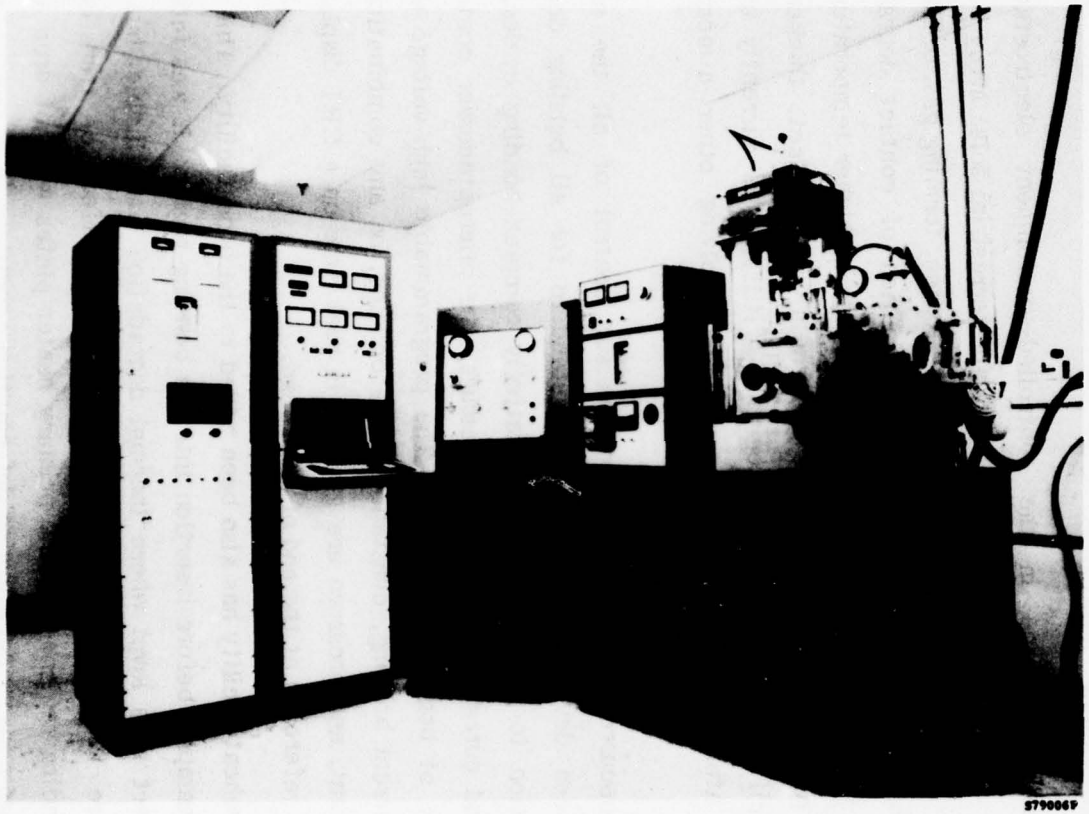

Figure 1. Controlled Environment, Microprocessor Controlled Electrostatic Bonder

Total process cycle time is limited by the vacuum pump-down time required to produce a clean bond environment. Cassettes of five samples have been in use to reduce the bonding cycle time. Five samples from a cassette can be bonded sequentially without breaking the environment. A second cassette can be prepared while the first is being processed. A considerable increase in sample throughput has been achieved. A new system for cell/cover glass alignment has been developed and tested during this program. This new jigging has two features. First, it places the cover glass on the bottom of the bonding stack rather than on top. Although some heating is from above, the primary heating is from below. This change reduces the cell's exposure to thermal degradation. The second feature of this jigging is improved dimensional flexibility. The edge of the cell with the contact bar is the reference edge. The cover glass is recessed from this edge by a ledge of prescribed dimension. Movable wedges index the cell and cover glass against the reference points. Thus, by precisely controlling only one jig dimension, cells varying by several mils in overall size can be handled in a single fixture.

Another fixture variation which has been partially implemented is the use of pressure domes and ceramic electrodes of lower thermal mass. Low thermal mass domes and electrodes decrease the temperature drop on sample insertion into the bond area, and also allow the sample temperature to change more rapidly after insertion.

3.1.2 Sample Temperature Profiling

To perform temperature profiling tests, a 0.010-inch-thick cover slip and a silicon wafer, both 2 cm square, were bonded together with a fine wire thermocouple trapped between them. This assembly, closely duplicating a real solar cell bonding configuration, was placed in a standard experimental setup and put through a variety of bonding cycles. A typical cycle is shown in Figure 2. Table 2 gives heating rate data, both in degrees and in percent of set-point temperature. Included in this listing is the viscosity of the glass at the indicated temperatures and a more convenient measure of glass softness, the reciprocal of the viscosity expressed as a percentage of the maximum value. Several conclusions can be drawn from these temperature profile data:

1. Sample equilibrium temperature and bonder set-point temperature are the same, at least to within measurement accuracy.

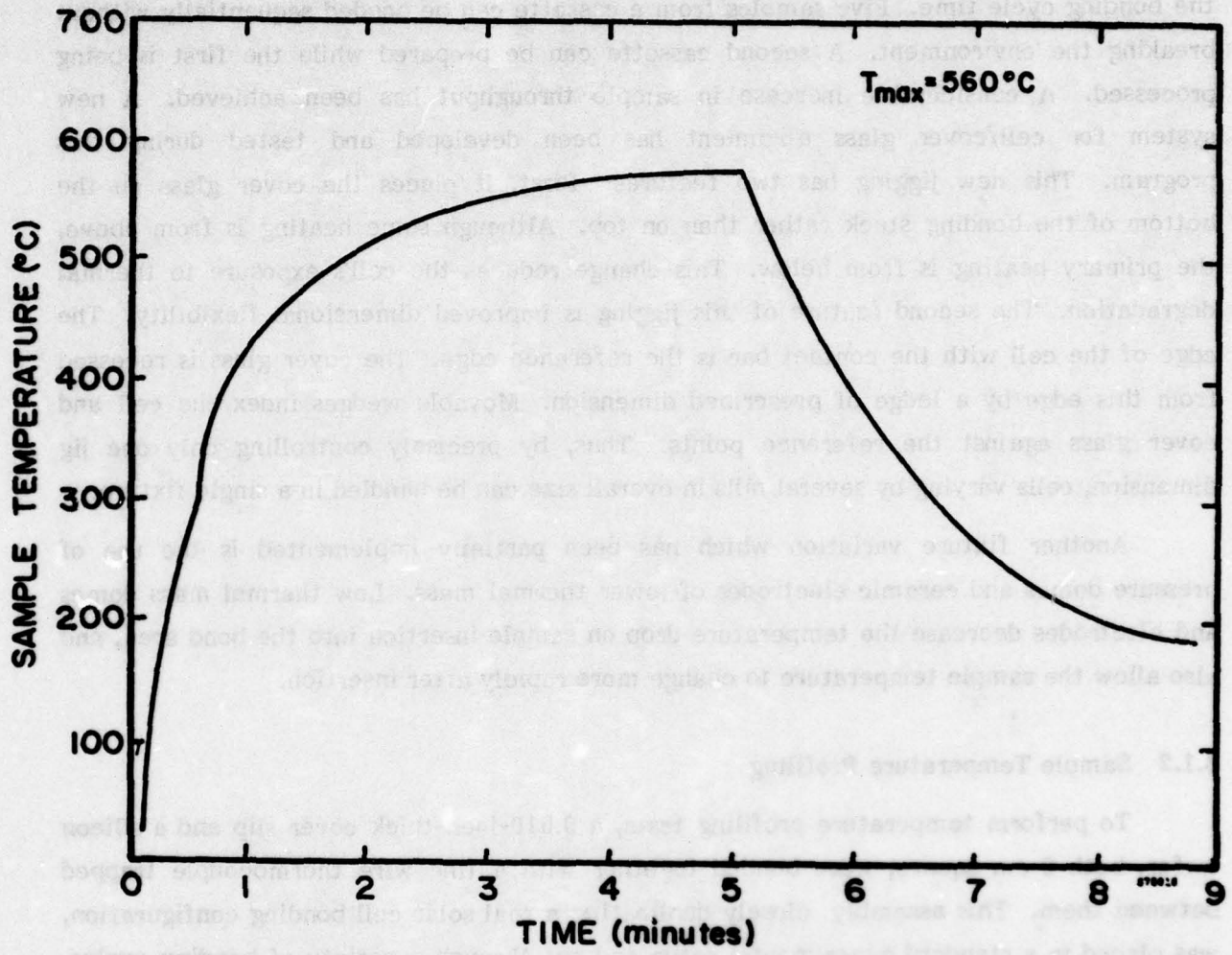

TIME(min.)	PRESSURE
0	0
1/2	CONTACT
1 1/2	P1
2	P max
4 1/2	0
5	WITHDRAW SAMPLE

Figure 2. **Solar Cell Temperature Profile During a Typical Electrostatic Bonding Cycle (Set-Point Temperature, 560°C)**

2. The sample reaches maximum temperature in approximately 4 1/2 minutes.

3. The shape of the heating curve greatly affects the total required bonding time.

This last point can be seen by looking at the time interval between 3 and 4 1/2 minutes. Over this range the temperature rises only 3 percent while the glass viscosity decreases by a factor of three. This slow heating exposes the cells to considerable thermal degradation before the glass approaches its softest condition. A steeper heating cycle might allow significantly shorter bonding cycles.

TABLE 2
HEATING RATE DATA FOR A TYPICAL SPACECRAFT SOLAR CELL ELECTROSTATIC BONDING CYCLE

$T_{set} = 560^{o}C$

Time (min)	Temperature (^{o}C)	Percent of T_{set}	Glass Viscosity (Poise)	$1/\eta$ (% of maximum)
0	37	6.6	-	-
1/2	288	51.4	-	-
1	424	75.7	6.6×10^{15}	0.002
1 1/2	485	86.6	2.7×10^{13}	0.4
2	515	92.0	2.7×10^{12}	3.7
2 1/2	533	95.2	6.0×10^{11}	17
3	542	96.8	3.2×10^{11}	32
3 1/2	548	97.8	2.3×10^{11}	43
4	555	99.1	1.3×10^{11}	79
4 1/2	559	99.8	1.0×10^{11}	100
5	560	100.0	1.0×10^{11}	100

The heating rate of samples in the bonder facility with the added preheat table was tested for several bond cycles. For best deformation with minimum degradation, it is necessary to bring the sample up to bonding temperature as rapidly as possible. Figure 3 compares the temperature rise of samples subjected to the six different bond cycles listed in Table 3. Two major variations of the cycle are made. First, tests are tried using a two-temperature bond cycle, wherein the temperature of the bottom heater starts high and is lowered to the final bond temperature during the process. Second, samples are tried with preheats of 20°C, 230°C, and 350°C. Figure 4 shows the same data plotted in terms of inverse viscosity, a measure of glass softness. It can be seen that:

1. The 350° preheat brings the glass to a given level of softness 40 to 50 seconds sooner than the corresponding cycle without preheat. The 230° preheat helps only marginally, if at all.
2. Two-temperature cycles result in a steeper viscosity versus time curve. This effect is more apparent in the 40° offset case than the 20° offset.

Of the cycles tested, Cycle III showed the greatest likelihood for a low-degradation bond. From Figure 4, it is clear that this cycle rises most rapidly through the region of high viscosity to the region where deformation is possible. Further testing focused on cycles with large temperature offset similar to the ones reported here.

A third set of temperature/time profiles was taken for several bond cycles. The physical parameter changes studied included:

1. Use of modified pressure domes with lower thermal mass
2. Use of modified pressure domes in conjunction with smaller (lower thermal mass) ceramic electrodes
3. Helium atmosphere
4. Vacuum

The bond process parameters studied were the effects of a large temperature offset in two-temperature bonds, and the effects of preheat in conjunction with two-temperature bonds.

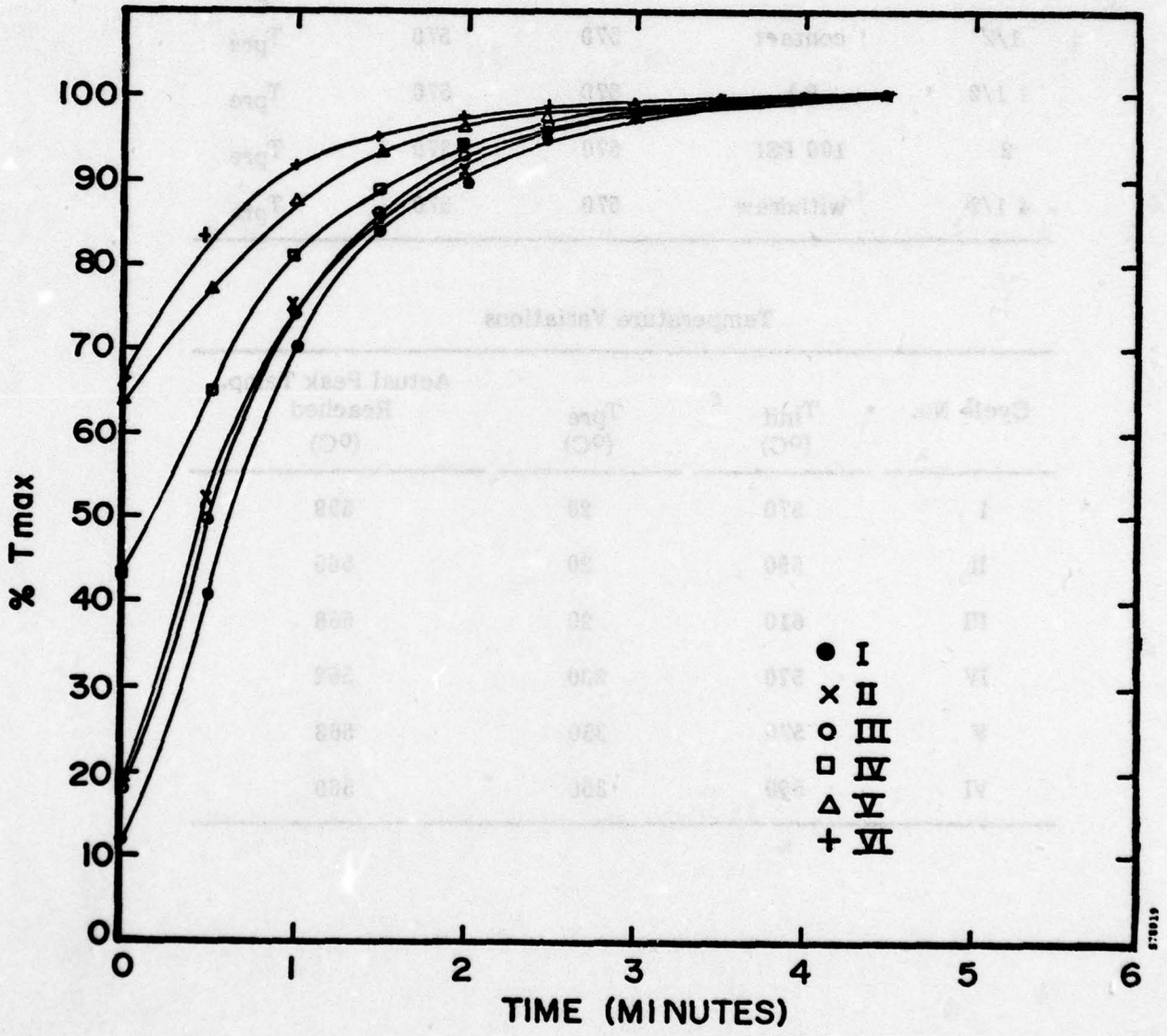

Figure 3. Temperature Versus Time for Six Cycle Variations

TABLE 3
BOND CYCLES USED IN TEMPERATURE PROFILE EXPERIMENTS

Basic Cycle

Time (min)	Pressure	T_{top} (°C)	T_{bot} (°C)	T_{pre} (°C)
0	0	570	T_{init}	T_{pre}
1/2	contact	570	570	T_{pre}
1 1/2	P ↑	570	570	T_{pre}
2	100 PSI	570	570	T_{pre}
4 1/2	withdraw	570	570	T_{pre}

Temperature Variations

Cycle No.	T_{init} (°C)	T_{pre} (°C)	Actual Peak Temp. Reached (°C)
I	570	20	559
II	590	20	565
III	610	20	568
IV	570	230	562
V	570	350	563
VI	590	350	569

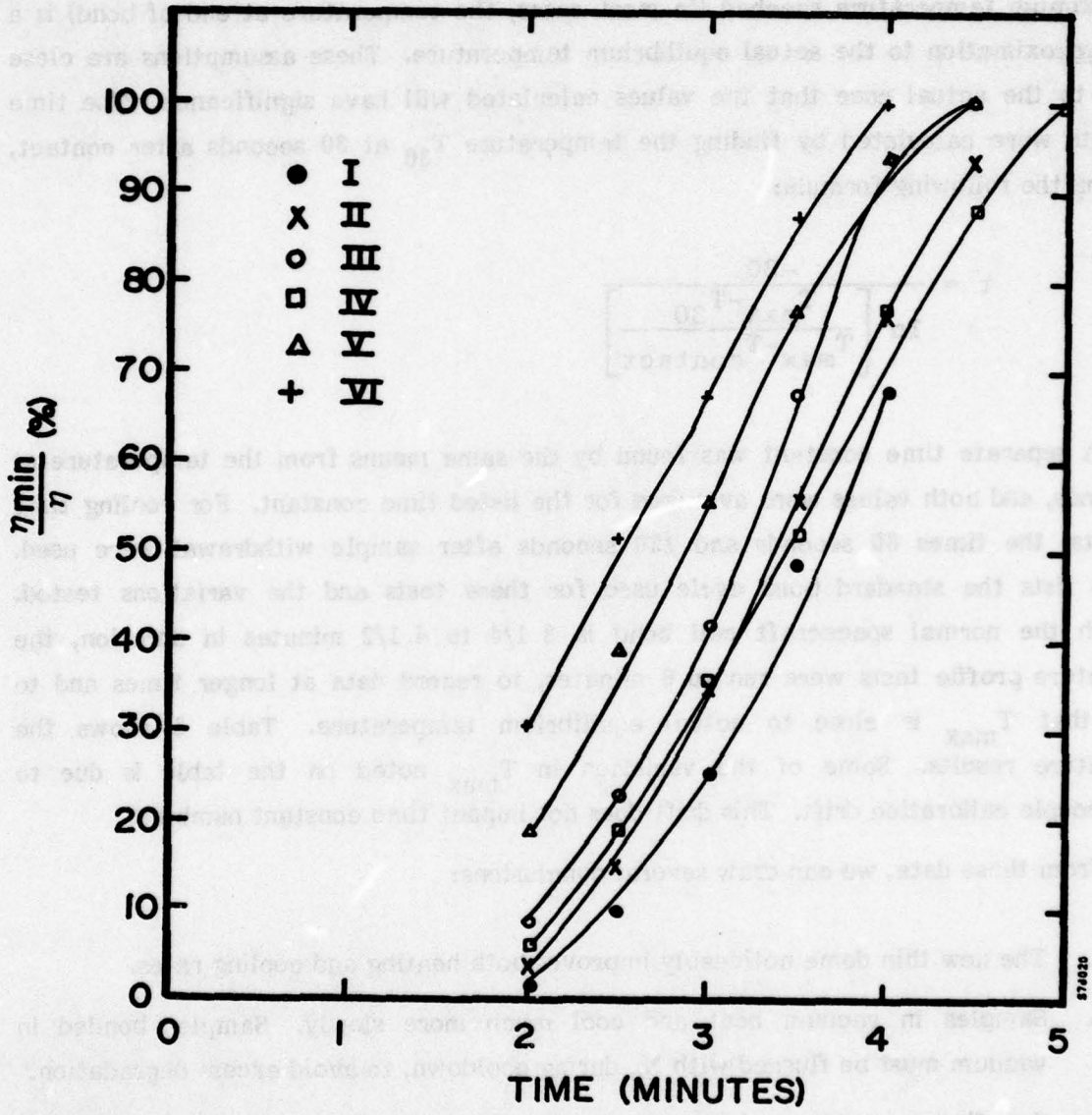

Figure 4. Inverse Viscosity Versus Time for Six Cycle Variations

Experimental data were reduced from temperature/time profile curves to a single characteristic time constant, for ease of data analysis. The time constant is the time it takes for the temperature to come to 1/e of the equilibrium value. This analysis was done under the assumptions that the data fit a single exponential profile curve and that the maximum temperature reached (in most cases, the temperature at end of bond) is a close approximation to the actual equilibrium temperature. These assumptions are close enough to the actual case that the values calculated will have significance. The time constants were calculated by finding the temperature T_{30} at 30 seconds after contact, and using the following formula:

$$\tau = \frac{-30}{\ln\left[\frac{T_{max}-T_{30}}{T_{max}-T_{contact}}\right]}$$

A separate time constant was found by the same means from the temperature at 60 seconds, and both values were averaged for the listed time constant. For cooling time constants, the times 60 seconds and 120 seconds after sample withdrawal were used. Table 4 lists the standard bond cycle used for these tests and the variations tested. Although the normal spacecraft cell bond is 3 1/4 to 4 1/2 minutes in duration, the temperature profile tests were run to 6 minutes, to record data at longer times and to assure that T_{max} is close to actual equilibrium temperature. Table 5 shows the temperature results. Some of the variation in T_{max} noted on the table is due to thermocouple calibration drift. This drift does not impact time constant numbers.

From these data, we can draw several conclusions:

1. The new thin dome noticeably improves both heating and cooling rates.
2. Samples in vacuum heat and cool much more slowly. Samples bonded in vacuum must be flushed with N_2 during cooldown, to avoid excess degradation.
3. A helium atmosphere heats and cools samples more rapidly than a nitrogen atmosphere during bond.
4. Temperature offsets have some advantage in heating rate.
5. 250°C and 300°C preheats have little impact on heating time constant. Residual heat slows down the cooling rate. For this reason preheating the sample is probably undesirable.

TABLE 4
BOND CYCLE FOR TEMPERATURE PROFILE TESTS

(1) Standard Cycle

t (min)	P	T_{top}	T_{bot}	T_{pre}
0	0	570°C	570°C	20°C
1/2	Contact	570°C	570°C	20°C
1 1/2	P↑	570°C	570°C	20°C
2	100 PSI	570°C	570°C	20°C
6	0	570°C	570°C	20°C

(2) Variations in bonder parameters*

(a) same cycle, modified pressure domes
(b) same cycle, modified domes and ceramic electrode
(c) same cycle, in vacuum
(d) same cycle, in helium

(3) Variations in bond cycle parameters

(a) Both heaters initially offset to 620°C, turned to 570°C at t = 30 sec
(b) Both heaters initially offset to 620°C, turned to 570°C at t = 2 min
(c) Both heaters initially offset to 620°C, turned to 570°C at t = 3 min
(d) Both heaters initially offset to 620°C, turned to 570°C at 30 sec
(e) Same as (d), 300°C preheat
(f) Bottom heater only offset to 620°C, turned to 570°C at 30 sec
(g) Top heater offset to 580°C, turned to 570°C at 30 sec
Bottom heater offset to 620°C, turned to 570°C at 30 sec

*Unless noted, all cycles used the standard (unmodified) domes and ceramic.

TABLE 5
TEMPERATURE PROFILING RESULTS

Cycle			T_{max} (°C)	Heating Time Constant (sec)	Cooling Time Constant (sec)
(1)	Standard 570°C cycle		538	40.7	227
(1)	repeated		571	43.0	234
(2)	a:	modified domes	544	27.8	178
(2)	b:	modified domes & electrode	548	27.5	163
(2)	c:	vacuum	560	64.7	861
(2)	d:	Helium	568	36.1	168
(3)	a:	620/570 at 30 sec	618	35.4	244
(3)	a:	repeated	610	35.7	260
(3)	a:	repeated	600	36.0	254
(3)	b:	620/570 at 2 min.	603	36.5	253
(3)	c:	620/570 at 3 min.	607	39.0	237
(3)	d:	620/570, 250°C preheat	599	36.0	278
(3)	e:	620/570, 300°C preheat	598	37.7	331
(3)	f:	620/570, bottom only	583	36.5	265
(3)	g:	620/570 bottom, 580/570 top	586	36.6	232

Table 5 shows clearly that cooling rates are currently slow compared to heating rates, thus leaving open the possibility of considerable thermal degradation during cooling. This is due to an insulating plate added to the preheat/cooling chamber for annealing of terrestrial modules. This plate has been replaced by a thermally conductive graphite plate for cooling of spacecraft cells, starting with bonding on OCLI lot 9 (see Section 3.3). This replacement has effectively speeded cooling by directly coupling the cell to the water-cooled loading table. It may be possible to produce even faster cooling by running a continuous flow of gas over the cell during the cooling stage.

3.2 GLASS SELECTION

Glass selection is critical to the success of electrostatic bonding. Corning 7070 glass was chosen for its close thermal expansion match to silicon at bond temperatures, without which stress-free bonds are impossible.

Optical transmittance at short wavelengths for 7070 glass decreases with exposure to electron radiation. This darkening is bleached by exposure to ultraviolet radiation at solar constant intensities.[2,3] Flight experiment data show that electron induced darkening is comparable for 7070 and fused silica cover glasses. In particular, on the NTS-2 satellite after 225 days in an orbit with a predicted fluence of 1.2×10^4 1 MeV e^-/cm^2, cells with electrostatically bonded 7070 glass covers degraded at the same rate as control cells conventionally covered with 7940 fused silica.[4]

Previous tests have shown considerable variation among samples in electron induced darkening. Corning Glass Works attributes these differences to manufacturing process variations. Sheet 7070 has limited usage, so is fabricated in small, manually operated melting pots. The experience at Corning is that impurity variations of only a few parts per million can cause large differences in darkening characteristics. Compositional variations may be traceable to changes of suppliers of raw materials from which the glass is produced or to manual operations, especially stirring, within a melt.

To evaluate the induced darkening of the presently available 7070 and to select the best material for this program, Spire used the electron Dynamitron radiation facility at Hanscom Air Force Base. Three groups of nominally 10-mil-thick (254-μm) cover slips were exposed to 1-MeV electrons. The glass was fabricated from three different sources: 4-mm poured 7070, procured by Spire; 8-mm 7070 from a different Corning

melt, also procured by Spire; and OCLI stock 7070 from an unknown Corning melt. Six samples of each were irradiated at two fluences, 3×10^{14} e^-/cm^2 and 1×10^{16} e^-/cm^2. These are roughly equivalent to the fluences predicted for 5 and 150 years in 0° geosynchronous orbit, respectively.[5]

Optical transmittance before and after irradiation is shown in Figure 5. The stock of 8-mm glass retained significantly higher transmittance after irradiation. This batch-to-batch variation was markedly higher than the variation between samples within a single batch.

Samples showing the greatest and least darkening were delivered to Corning Glass Works for analysis. The least darkened glass was used for this program.

3.3 MULTIPLE-LAYER ANTIREFLECTION (MLAR) COATED CELL BASELINE

3.3.1 Solar Cell Experience

Work reported previously[3] showed the feasibility of applying ESB covers to solar cells. Two types of bonds have been made: bonds between a solar cell and a grooved cover, where the grooves in the glass accept the grid lines on the cell; and deformation bonds, where the glass of the cover is deformed around the grid lines during the bonding process.

The grooved covers have the advantage of requiring only short bonds at relatively low temperature, resulting in minimal degradation of the cell. However, the grooved covers require a high degree of consistency in the cell metallization pattern, including no excess or stray metal; perfect cell/cover registration; additional expense in manufacturing the covers; and limit contact geometries to linear, or at best, rectangular configurations. Deformation bonds, on the other hand, require more severe conditions in the way of bond temperature, time, and pressure to achieve low enough glass viscosity for significant deformation to occur. Such severe treatment can lead to cell degradation. However, deformation bonding is both less expensive and easily automatable, requires no constraints on cell metallization other than line height and spacing, and produces a truly integral structure. Deformation bonds have been demonstrated to have complete reliability under severe conditions and thermal stress. Thus, for this program, deformation bonds have been used exclusively.

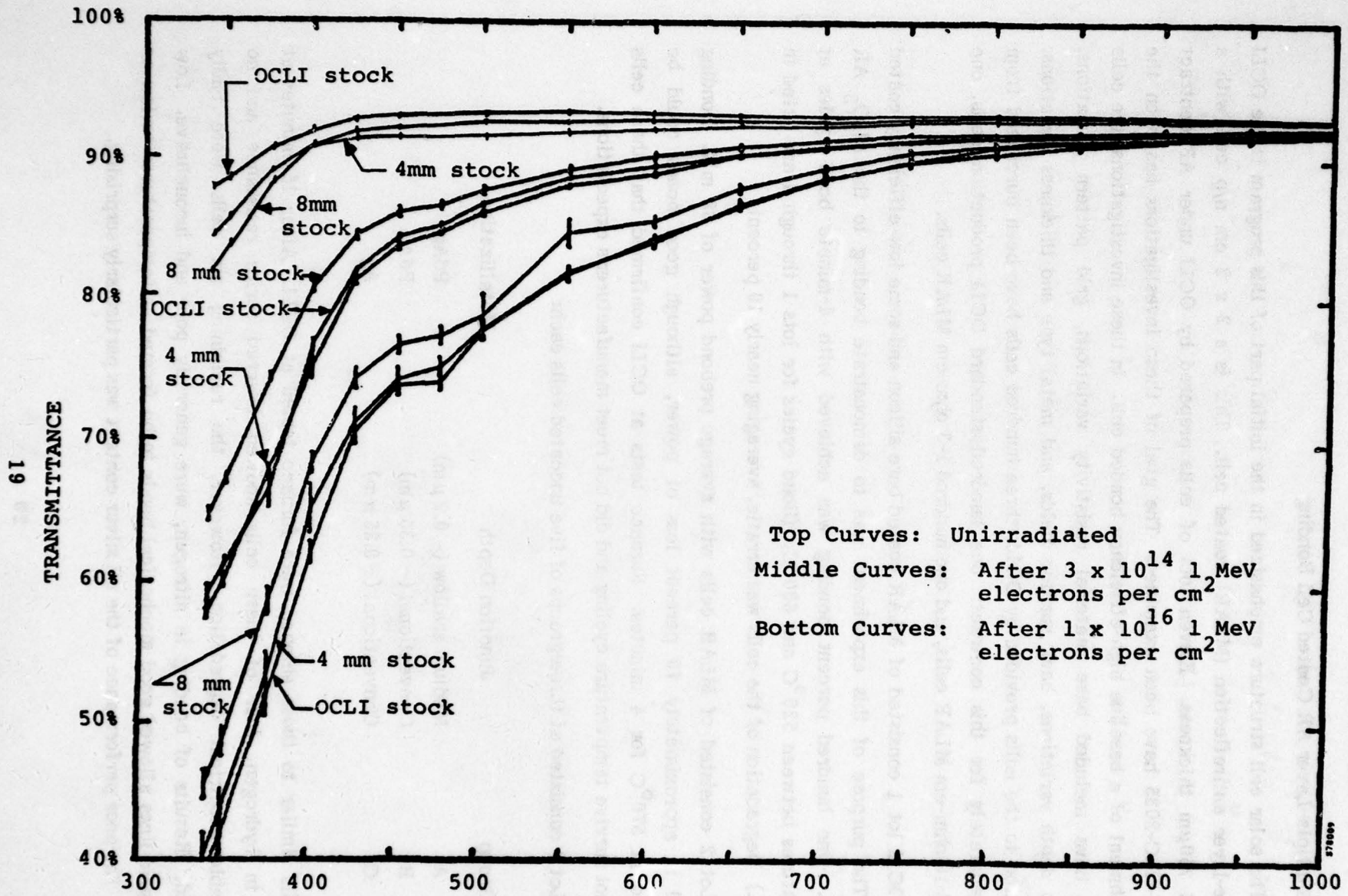

Figure 5. Optical Transmittance for Irradiated and Unirradiated 7070 Glass Coverslips

3.3.2 Multiple-Layer AR Coated Cell Bonding

The solar cell structure emphasized in the initial part of this program is the OCLI multiple-layer antireflection (MLAR) coated cell. This is a 2 x 2 cm n/p cell with a nominal 250μm thickness. Eleven lots of cells prepared by OCLI under AF contract F33615-77-C-2035 have been examined. The goal of these investigations has been the establishment of a baseline high-efficiency bonded cell. In these investigations, the cells studied have included base material resistivity variations, grid pattern variations, junction depth variations, back surface fields, and metal type and thickness variations. In addition to the cells provided by OCLI, three hundred cells have been purchased from OCLI separately for this contract: one hundred standard OCLI production cells, one hundred 10 ohm-cm MLAR cells, and one hundred 1-3 ohm-cm MLAR cells.

OCLI lot 1 consisted of MLAR coated bare silicon and some low-efficiency coated cells. The purpose of this experiment was to demonstrate bonding to the Al_2O_3 AR coating. One hundred percent bonding was achieved with 4-minute bond cycles at temperatures between 520°C and 600°C. (Bond cycles for lots 1 through 4 are listed in Table 6.) Degradation of the cells was erratic, averaging nearly 10 percent.

Lot 2 consisted of MLAR cells with average prebond power of 68 mW. Bonding resulted in approximately 70 percent loss of power, although good bonds could be achieved at 570°C for 4 minutes. Furnace tests at OCLI confirmed that these cells would not survive temperature cycling and did not meet manufacturer's expectations.

Lot 3 consisted of three groups of five uncoated cells each:

Group	Junction Depth	Metallization
A	Medium shallow (~ 0.2 μm)	PdAg
B	Conventional (~ 0.35 μm)	PdAg
C	Conventional (~ 0.35 μm)	Ag

Ten cells similar to those shipped were furnace tested at OCLI. After 15 minutes at 600°C in hydrogen, four of these cells showed lowered series resistance and no appreciable electrical degradation. However, the remaining six cells were badly degraded. Results of bonding in nitrogen, were generally poor and inconclusive. Low profile grid lines allowed good mechanical bonds to be formed at temperatures as low as 520°C. The poor performance of the all silver contact was particularly surprising.

TABLE 6
BOND CYCLES FOR OCLI LOTS 1 - 4

Lot	Time (min:sec)	Pressure (PSI)	Voltage (volts)	Temperature (°C)
1	0	0	0	Varied:
	1:00	80	0	520-600
	1:30	80	500	
	4:00	0	0	
2	0	0	0	570
	0:30	Contact	0	
	1:30	100	750	
	4:00	0	0	
3	0	0	0	Varied:
	0:30	Contact	0	520-550
	1:30	100	750	
	4:00	0	0	
4	0	0	0	550*
	0:30	Contact	0	
	1:30**	100	750	
	4:00**	0	0	

* Cell A-3 bonded at 520°C.

** For Cells B-28 and C-32 through -36, these times were increased 30 seconds to deform around closely spaced grid lines.

Since the cells were not AR coated, short circuit currents generally increased after bonding and I-V curve fill factors decreased accordingly. Bonds were made at various temperatures between 520°C and 550°C. Losses in open circuit voltage were minimal. The largest degradation was in a curve factor, where losses usually between 15 and 25 percent were experienced. Variable thermal performance of these cells was a problem. One bonded cell from group A showed only a 4 percent loss in curve factor, while another of this group lost 37 per cent after an identical bonding cycle.

One cell from each of the three groups was put through the 550°C bonding cycle without voltage or application of deformation pressure. Losses were generally less than those experienced with the full bonding cycle.

Lot 4 consisted of five groups of varied metallization pattern and material, AR coating, and surface finish (see Table 7). Prebond cell power ranged from 49.8 to 58.0 mW. All cells, with one exception, were bonded at 560°C. Average bonded area was 87 percent for the 24 cells bonded at 560°C. The chemically polished cells appeared to bond more uniformly across the main surface than did their mechanically polished equivalents. However, bonding at the edge of those cells was poor due to the "pillowing" caused by the chemical polish.

Electrical performance of the bonded cells, as measured by loss of maximum power, was down 6.7 percent for the group. Almost all the power loss was due to the decrease of curve factor. There were no statistically significant postbond differences among subgroups in the lot. Figure 6 shows the I-V curve of the one of these cells before and after bonding.

OCLI lot 5 consisted of 25 cells, bonded in groups of three (rather than individually), in at attempt to separate equipment related variation from cell-to-cell variation. Four variations of a basic bond cycle were used, as listed, with comments, in Table 8. Average prebond power for these cells was 62.2±0.7 mW. Postbond power averaged 57.2±2.1 mW. Bond results are listed in Table 9.

Cells bonded in cycle I show both large intra-run and large inter-run variations. The large inter-run variations, with small standard deviations, suggest equipment related effects. However, since the spread evident within a run is often as large as these inter-run variations, it cannot be said that equipment reproducibility is definitely a problem. Made evident by mixed bonding results within a group and by the large amount of sample breakage is the difficulty of multiple-cell bonding. These poor bonding results are attributable at least in part to nonuniform contact pressure applied to the multiple

TABLE 7
CHARACTERIZATION OF OCLI LOT 4 CELLS

Group	Metallization		AR Coating	Preparation	Power (mW)
	Pattern	Material			
A	3 lines/cm	TiAg	SiO_2	Mechanical Polish	56.4±1.1
B	6 lines/cm	TiPdAg	Ta_2O_5	Mechanical Polish	55.2±1.3
C	6 lines/cm	TiPdAg	Ta_2O_5	Chemical Polish	51.1±0.2
D	4 lines/cm	TiPdAg	Ta_2O_5	Mechanical Polish	54.4±1.0
E	4 lines/cm	TiPdAg	Ta_2O_5	Chemical Polish	50.1±0.5

cell configurations. Any run-to-run variations that might be present are masked by this intra-run equipment nonuniformity. Much more development work and possibly facility modifications would probably be necessary if significant improvements in multiple cell bonding are to be achieved. Figures 7 and 8 present pre- and postbond I-V curves of cells representing the best and worst case results obtained from lot 5.

MLAR lot 6 consisted of high efficiency cells. These cells were expected to degrade thermally, however it was hoped that degradation would be small and postbond power would be high. Thermal tests at OCLI predicted degradation of 7 percent after exposure to 570°C for 10 minutes.

Grid pattern heights on these cells were large but variable so that poor bond coverage was attained. Cells bonded with full pressure and voltage typically lost 19 percent of their prebond power. Part of this loss is due to a decrease in incident light caused by reflection at unbonded interfaces. When correction was made for this factor, cell performance loss was calculated at 14 percent. Three cells were bonded without voltage and deformation pressure. Power loss for these cells averaged 4.4 percent, consistent with the OCLI thermal test data. These data indicate an additional degradation cause, apparent as both curve factor loss and short circuit current loss, and separate from thermal degradation. This degradation is inherent in either voltage, pressure, or glass cover. Bond cycles are listed in Table 10.

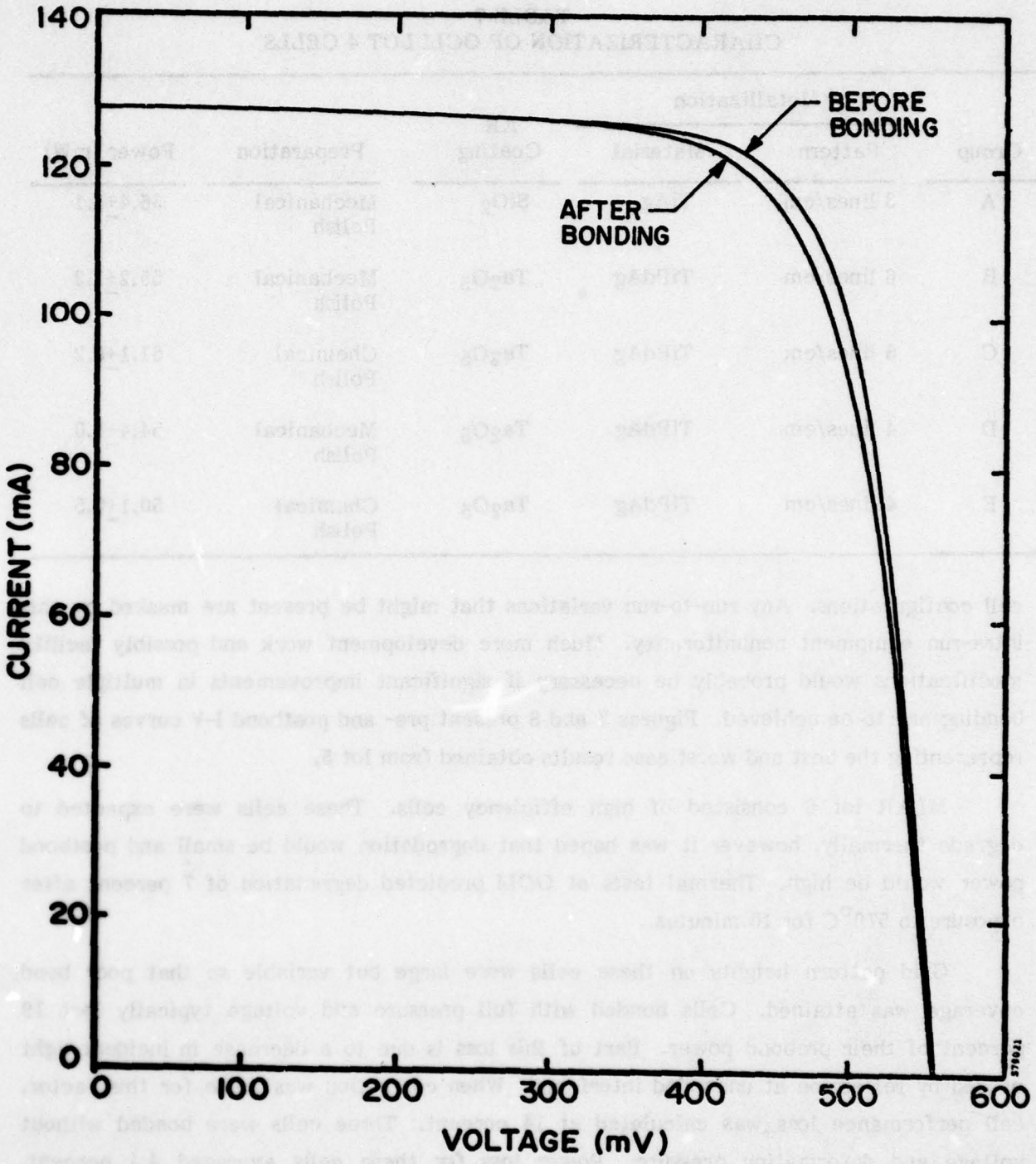

Figure 6. I-V Curves, Before and After Bonding, for OCLI Lot 4 Cell D-68 Under 135 mW/cm^2 Tungsten Light

TABLE 8
BOND CYCLES USED ON OCLI LOT 5

Cycle Number	Bond Parameters	Number of Runs	Results	Recommendations
I	T = 560°C t = 4.5 min	4	Bonding moderate to poor except one run. Degradation mixed but too high.	Test effects of lower temperature and longer time.
II	T = 550°C t = 6.5 min	1	Excellent bonding. Severe degradation.	Try shorter time.
III	T = 550°C t = 5.5 min	2	Good bonding. Too much degradation.	Test effects of higher temperature and shorter time.
IV	T = 570°C t = 4.0 min	1	Poor bonding. Same degradation as in III.	Need short low-temperature cycle, thus faster preheat.

Note: Cells bonded in groups of three.

TABLE 9
BOND RESULTS FOR OCLI LOT 5

Cell No.	Bond Temp (°C)	Bond Time (min)	Bond Area (%)	Electrical Changes (%)				Notes	Bond Cycle (See Table 8)
				V_{oc}	I_{sc}	CFF	P_{max}		
5-1	-	-	-	-	-	-	-	Control Cell	
5-2			40	-0.8	-4.9	-2.6	-7.3		
5-3	570	4.0	60	-0.8	-8.3	-3.9	-11.3		IV
5-4			95	-0.8	-3.4	-66	-9.7	(1)	
Avg	570	4.0	65	-0.8	-5.5	-4.4	-9.4±2.0		
5-5			80	-1.0	0	-4.0	-7.0		
5-6	550	5.5	85	-1.0	-5.0	-3.0	-8.0		III
5-7			100	-2.0	-5.0	-11.0	-9.0	(1)	
Avg	550	5.5	88	-1.3	-3.3	-6.0	-8.0±1.0		
5-8			100	0	-6.0	-1.0	-8.0		
5-9	550	5.5	95	-0.8	-3.4	-9.2	-12.7	(1)	III
5-10			100	0	-4.1	-5.3	-9.7	(1)	
Avg	550	5.5	97	-0.3	-4.5	-5.2	-10.1±2.4		
5-11			100	-0.8	-4.7	-13.3	-18.0	(1)	
5-12	550	6.5	100	-1.7	-4.8	-13.3	-18.5	(1)	II
5-13			100	0	-3.4	-8.0	-11.5		
Avg	550	6.5	100	-0.8	-4.3	-11.5	-16.0±3.9		
5-14			85	0	-4.8	-1.3	-3.2		
5-15	560	4.5	70	-0.8	-4.1	-1.3	-6.3		I
5-16			85	0	0	-2.6	-6.5	(2)	
Avg	560	4.5	80	-0.3	-3.0	-1.7	-5.3±1.9		
5-17			100	-0.8	-2.1	-5.3	-11.5	(1)	
5-18	560	4.5	95	-0.8	-1.4	0	-3.3		I
5-19			100	-1.6	-2.0	-8.5	-13.0		
Avg	560	4.5	98	-1.1	-1.8	-4.6	-9.3±5.2		
5-20			85	-0.8	-2.8	-7.8	-14.0	(1)	
5-21	560	4.5	10	Broken before testing					I
5-22			95	-1.7	-5.4	-6.6	-12.7		
Avg	560	4.5	63	-1.3	-4.1	-7.2	-13.4±0.9		
5-23			100	-0.8	-4.1	-7.8	-11.0	(1)	
5-24	560	4.5	60	-0.8	-4.1	-5.3	-15.0	(2)	I
5-25			20	-0.8	-4.3	-2.7	-6.4	(1)	
Avg	560	4.5	60	-0.8	-4.2	-5.3	-10.8±4.3		
Average, All Cells			82	-0.8	-3.8	-5.7	-10.2		
Average, Uncracked Cells			83±19	-0.8±0.6	-4.1±2.3	-4.2±2.9	8.3±3.4		

Notes: (1) Cell or glass or both cracked.
(2) Arcing during bonding.

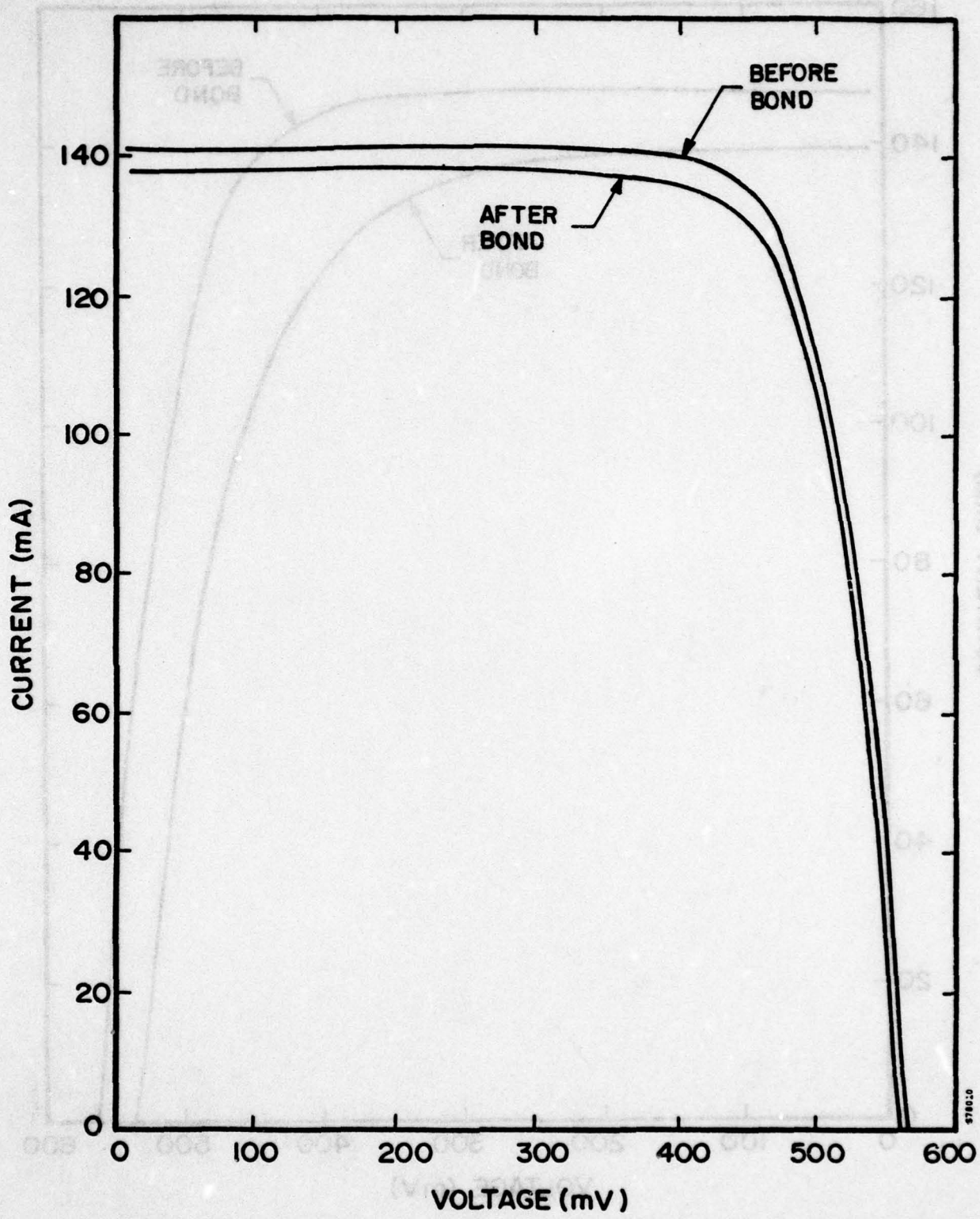

Figure 7. AM0 I-V Curves, Before and After Bonding, For OCLI MLAR Cell 5-18

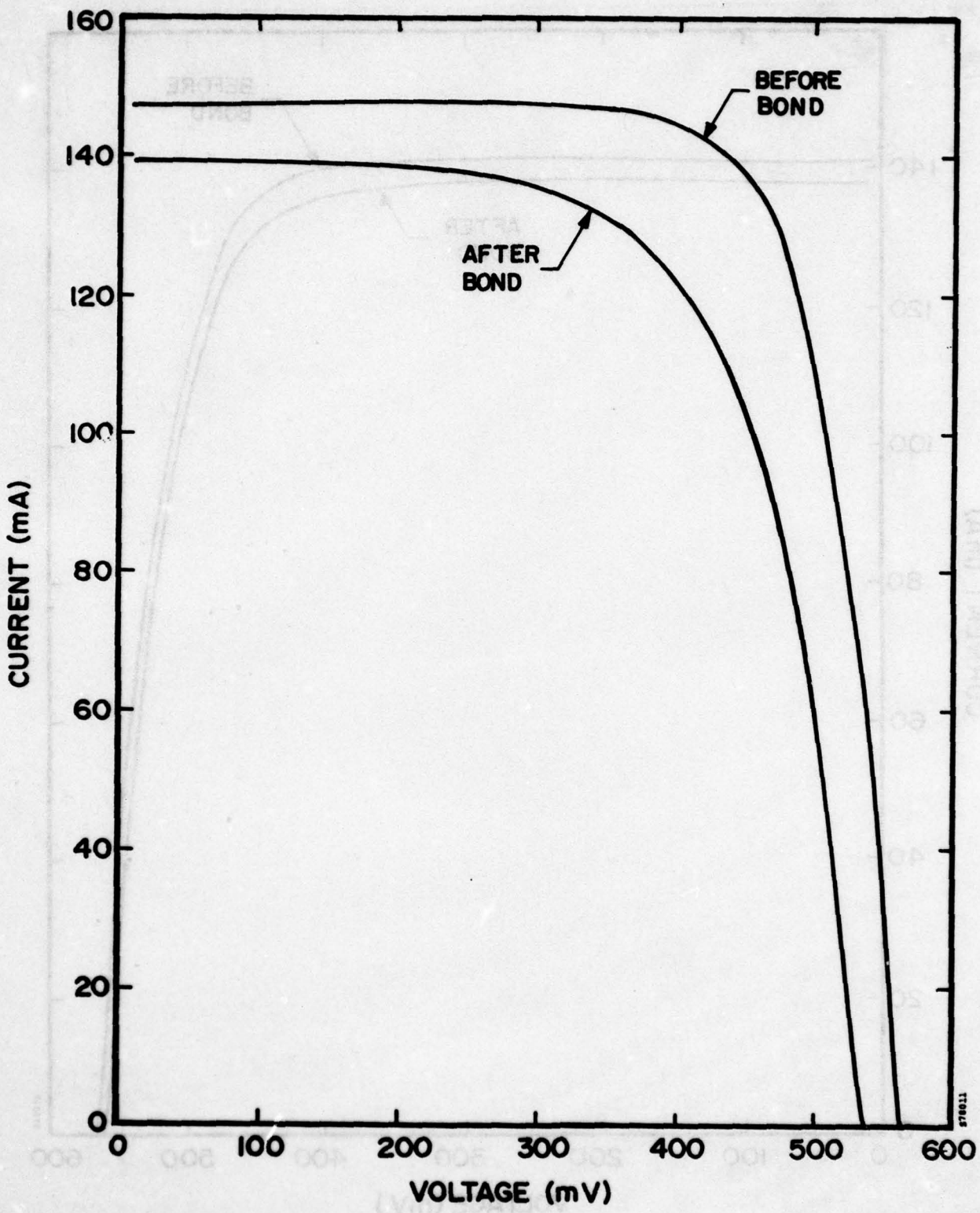

Figure 8. AM0 I-V Curves, Before and After Bonding, for OCLI MLAR Cell 5-12

TABLE 10
BOND CYCLES FOR OCLI LOTS 6 AND 7

Lot	Time (min:sec)	Pressure (PSI)	Voltage (volts)	Temperature (°C)
6	0	0	0	570
	0:30	Contact	0	570
	1:00	P ↑	0	570
	2:00*	100	500	570
	4:30*	0	0	570
7				
Cycle 1	0	0	0	570
	0:30	Contact	0	570
	2:00	P ↑	0	570
	2:30	100	750	570
	4:30	0	0	570
Cycle 2	0	0	0	570
	0:30	Contact	0	570
	2:00	P ↑	0	570
	3:00	100	750	570
	5:00	0	0	570
Cycle 3	0	0	0	570
	0:30	Contact, P ↑	0	570
	2:00	90 ↑	0	570
	2:30	120	750	570
	4:30	0	0	570
Cycle 4	0	0	0	570
	0:30	Contact, P ↑	0	570
	2:00	90 ↑	0	570
	2:30	150	750	570
	4:30	0	0	570

After lot 6 bonding, 100 OCLI production spacecraft cells were obtained and bonded, to verify that no equipment shifts that might be contributing to degradation had occurred and to test degradation modes on standard cells. This work is reported separately in Section 3.3.3.

Lot 7 again consisted of three groups, all shallow junction cells. Group A had no AR coating and vanadium-silver metallization, while groups B and C had standard TiPdAg metal with MLAR. Group B used 2 ohm-cm material, and C used 10 ohm-cm material with aluminum alloy Back Surface Field (BSF). Due to the high metallization, the bond cycle was varied to include longer times and higher pressures (see Table 10). Both A and B degraded highly, while C, the high resistivity BSF cells, had less degradation and high postbond power, although the best cell of this lot showed only a 75 percent bond. The before and after bond I-V curve for this cell, with an after-bond efficiency of 12.2 percent, is shown in Figure 9. These results were encouraging enough to continue tests with high resistivity BSF cells in lots 10 and 11, although the nominal baseline (lot 8) became the low resistivity cell.

MLAR lot 8 consists of cells fabricated to the specifications arrived at during a technical meeting at AFAPL on 24 April 1978. These are the nominal baseline cells for this program. Cell characteristics are listed in Table 11. Prebond efficiency is 12.5 percent. These cells were to be used to demonstrate the program baseline of 62 mW or greater postbond power, with 90 per cent or better bond coverage. This cell specification is listed in Appendix A.

The original intent was to bond all these cells at a fixed cycle; however, during the experiment it was decided to change the bond schedule to achieve more uniform, higher coverage bonds. A change was made to a two-temperature bond cycle due to the results from temperature profile tests which showed a faster rise to sample temperature, enabling time to be cut off the bond cycle. This change had the immediate effect of both increasing bond coverage and decreasing degradation by a factor of two. Further shortening of bond time decreased cell power, although not to the levels of the original cycle. Post-bond data on these cells are reported in Table 12. The results obtained from cycle 2 were particularly encouraging in terms of consistency of both bond coverage and postbond power.

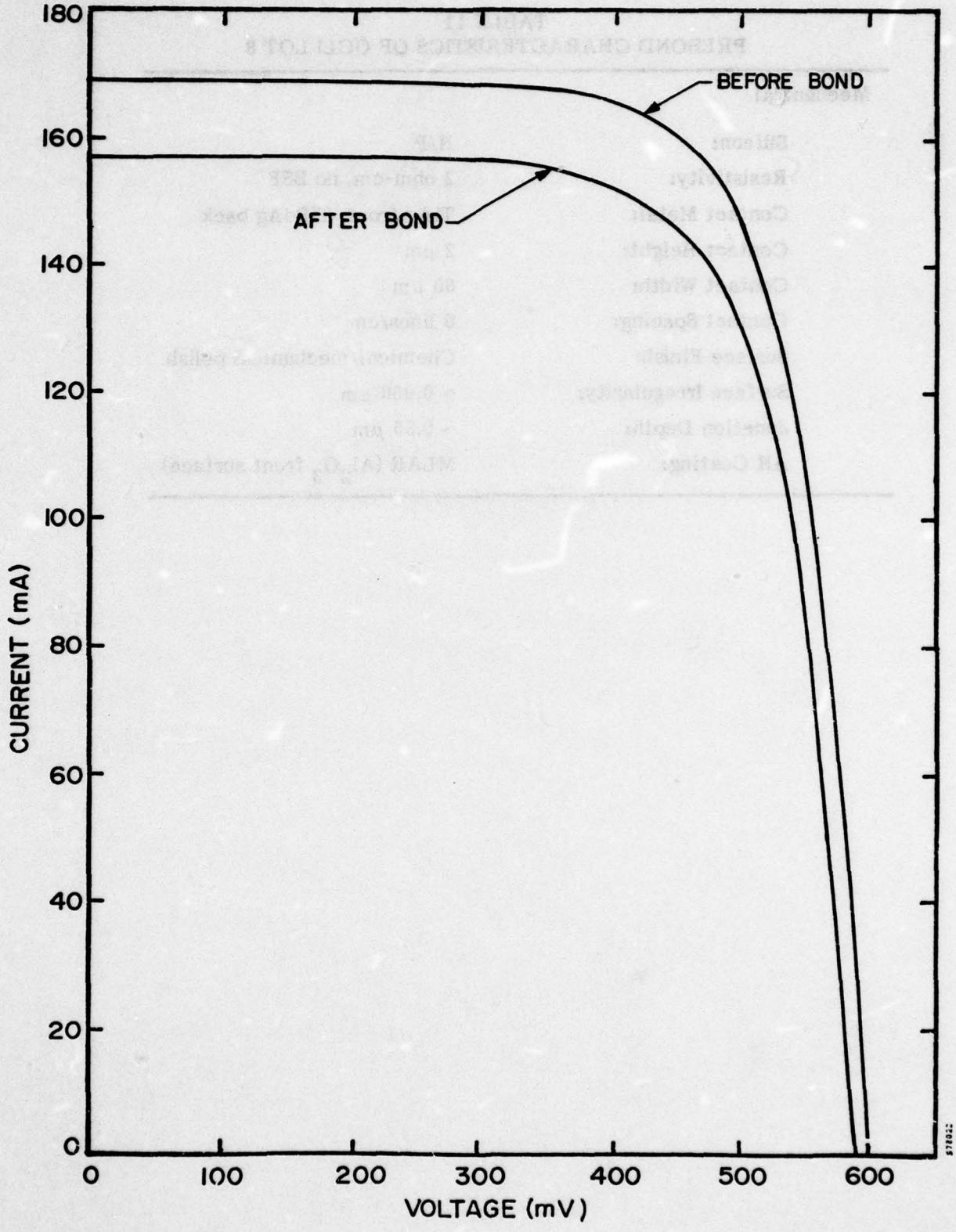

Figure 9. Pre- and Postbond I-V Curves, OCLI Lot 7C Cell 10A

TABLE 11
PREBOND CHARACTERISTICS OF OCLI LOT 8

Mechanical	
Silicon:	**N/P**
Resistivity:	**2 ohm-cm, no BSF**
Contact Metal:	**TiAg front, TiPdAg back**
Contact Height:	**2 μm**
Contact Width:	**60 μm**
Contact Spacing:	**6 lines/cm**
Surface Finish:	**Chemical/mechanical polish**
Surface Irregularity:	**$\sim$0.050 μm**
Junction Depth:	**$\sim$0.35 μm**
AR Coating:	**MLAR (Al_2O_3 front surface)**

TABLE 12
OCLI LOT 8 BOND MEASUREMENTS

Cycle	Cell No.	Percent Change From Prebond Measurements				% Bond	After-Bond Power (mW)
		V_{oc}	I_{sc}	P_m	CFF		
1	3	-1.3	-2.1	-6.0	-2.7	90	64.0
	16	-0.5	-0.7	-20.7	-19.9	100	52.8
	21	-0.5	-3.4	-38.6	-36.0	95	41.4
	23	0.0	-3.4	-5.9	-3.3	85	64.0
	24	-4.2	-6.9	-29.6	-21.2	100	46.9
	*25	-26.7	-61.4	-87.6	-56.4	80	8.4
	Ave.(5 cells)	-1.3±1.7	-3.3±2.3	-20.2±14.4	-16.6±14.0	94±7	53.8±10.1
2	4	0	-2.0	-5.9	-4.0	100	62.5
	5	0	-1.4	-9.4	-8.1	100	61.9
	6	-1.2	0.0	-17.4	-16.3	100	54.2
	** 7	-6.8	-43.0	-77.9	-58.4	100	15.2
	17	+1.2	-1.7	-5.3	-4.8	100	64.3
	18	-0.3	-2.7	-11.3	-8.5	95	61.4
	Ave.(5 cells)	-0.06±0.86	-1.6±1.0	-9.9±4.9	-8.3±4.9	99±2.2	60.9±3.9
3	8	0	-2.0	-12.9	-11.0	100	58.1
	9	0	-2.7	-6.2	-3.5	80	63.9
	10	-1.3	-4.0	-9.4	-4.4	80	63.8
	***11	-1.3	-2.7	-32.3	29.4	100	42.9
	12	0	-2.7	-11.8	-9.4	100	60.5
	13	-0.8	-27.2	-44.8	-23.4	75	38.4
	14	0	-2.7	-5.6	-3.0	100	63.9
	Ave.(6 cells)	-0.35±0.56	-6.9±10.0	-15.1±14.8	-9.1±7.7	89±12	58.1±9.9
4	15	-1.2	-1.3	-9.5	-7.1	100	60.6
	+19	-1.8	-4.1	-21.6	-15.1	100	61.5
	20	-1.3	-2.8	-9.8	-5.9	90	53.0
	Ave.(2 cells)	-1.2±0.7	-2.1±1.1	-9.7±0.2	-6.5±0.8	95±7	56.8±5.4
Ave. (18 cells)		-0.63 ±1.1	-3.87 ±6.0	-14.45 ±11.7	-10.7 ±9.2	93.9 ±8.5	57.5 ±8.1

* This cell removed from average due to atypical performance

** Cells shows evidence of arcing onto contact bar

*** Cell chipped after bond

\+ Cell cracked

The program baseline was established by these cells. Eight cells out of twenty-two met the after-bond power specifications, fifteen met the bond coverage specifications, and four cells met both specifications. Two cells, 9 and 10, were cycled from liquid nitrogen into 100°C water to test bond quality; the bond did not degrade. At this point, only the yield of high-efficiency bonded cells was thought to be a major problem. Improving the yield has proven to be more difficult than originally thought, partly because of changes in the bonder due to maintenance and partly because of the small numbers of baseline cells received after lot 8.

OCLI lot 9 consisted of two groups of 20 cells. Group A were 1-3 ohm-cm cells similar to lot 8, but with slightly lower power, while Group B were 10 ohm-cm cells similar to lot 7C. These cells were tested four times before bond to check measurement consistency. Except for a difference between the OCLI and Spire measurements of short circuit current and the resulting maximum power (the OCLI measurement being 3.6 percent higher), all measurements were consistent to three places. The difference between the OCLI and Spire measurements of P_{max} is probable due to differences in the standard cell used to calibrate the simulator. The lower measurement, Spire's, was used for all the reported results.

Bonding of lot 9 cells was poor, both mechanically and electrically. Only one cell met the baseline of 90 percent or better bond and 62+ mW postbond power. Cells in lot 9B had problems with large-scale irregularities in the back surface, due to lumps in the aluminum applied for the back surface field. This caused difficulties in bonding. Other bond difficulties resulted from modifications in the bonder during maintenance. Modified bond cycles for this lot, and lots 10 and 11, are shown in Table 13.

Lot 10 consisted of more high-efficiency 10 ohm-cm cells. Due to closely spaced, thick grid lines and slightly larger cell dimensions, the bonding of these cells was difficult. Very high pressure was needed for deformation, causing difficulties with cell cracking. Postbond power on these cells, however, was high, averaging 63 mW.

Lot 11 also consisted of 10 ohm-cm cells. Group 11B consisted of high efficiency cells with relatively high (5 μm) grid lines. Group 11A consisted of slightly lower efficiency cells with 2.5 μm grid lines. Table 14 shows bond results for these cells. Both cell groups had good postbond power: lot 11A yielded six cells out of fifteen of 63 mW or greater postbond power, while lot 11B yielded seven out of fifteen. Six of these cells had better than 90 percent bond coverage, averaging 65 mW with 98 percent bond. The greater yield was from lot 11A, with lower grid height.

TABLE 13
BOND CYCLES, OCLI LOTS 9, 10, AND 11

	Time (min:sec)	Pressure (PSI)	Voltage (volts)	Temperature (^{o}C)
Lot 9	0	0	0	590
Initial	0:30*	Contact	0	570
Schedule	1:30*	P↑	0	570
	2:00	100	750	570
	4:00	0	0	570
Lot 9	0	0	0	600
Initial	0:30	Contact	0	580
Schedule	1:30	P↑	0	580
	2:00	100	750	580
	4:00	0	0	580
Lot 10	0	0	0	600
and 11	0:30	Contact	0	580
Initial	1:00	65	0	580
Schedule	1:30	65↑	0	580
	2:00**	100**	750	580
	4:00	0	0	580
Lot 10	0	0	0	600
and 11	2:00	Contact	0	600
Final	2:30	65	0	600
Schedule	3:00	65↑	0	600
	4:00	165	0	600
	4:30	165	750	600
	6:30	0	0	600

TABLE 14
BOND RESULTS, LOT 11

Cell	Cycle Variations	% Change V_{oc}	% Change I_{sc}	% Change P_{max}	% Change CFF	Post-Bond Power	% Bond	Comments
Lot 11A								
A1	100 PSI	-1.03	-9.09	-11.6	-1.83	60.2	30	
A2	140 PSI	-1.36	-7.10	-10.4	-2.27	61.1	70	
A3	175 PSI	-2.91	-8.97	-12.4	-0.81	58.9	75	Cracked
A4	175 PSI	-0.86	-3.25	-17.2	-13.7	57.2	98	Hydraulics stuck, cell cracked
A5	5:30/165 PSI/ 600°C	-0.68	-3.84	-12.2	-7.93	62.0	88	
A6	"	-0.34	-1.93	-5.57	-3.30	64.4	100	
A7	"	-0.68	-5.84	-8.14	-1.79	64.3	20	Glass cracked
A8	"	-2.63	-14.2	-26.0	-11.7	50.0	30	Short circuit, cell cracked
A9	"	-3.55	-5.80	-14.0	-5.29	59.4	60	Cover bonded over output terminals, cell cracked
A10	"	-2.24	-10.0	-15.0	-3.37	58.3	20	
A11	"	-0.34	-7.00	-10.1	-3.11	63.0	98	
A12	"	-0.34	-3.82	-6.76	-2.70	66.2	85	
A13	"	-0.52	-5.69	-8.83	-2.91	63.0	60	
A14	"	-0.69	-3.24	-8.83	-5.18	63.0	100	
A20	"	-0.68	-2.60	-6.85	-3.76	65.3	98	
Average (uncracked cells)		-0.82 ±0.60	-5.43 ±2.78	-9.61 ±2.86	-3.64 ±1.76	62.6 ±2.4	74.9 ±29.6	

TABLE 14
BOND RESULTS, LOT 11
(Concluded)

Cell	Cycle Variations	% Change V_{oc}	% Change I_{sc}	% Change P_{max}	% Change CFF	Post-Bond Power	% Bond	Comments
Lot 11B								
B4	100 PSI	-1.66	-7.0	-12.7	-4.02	63.7	30	Glass cracked
B1	175 PSI/ vacuum	—	—	—	—	—	5	Cover cracked, broken after bond
B2	175 PSI (N_2)	—	—	—	—	—	90	Cover cracked, broken after bond
B3	175 PSI (N_2)	-0.50	-3.26	-5.32	-1.15	67.6	80	
B5	4:30/175 PSI	-6.76	-7.64	-21.5	-8.82	58.4	95	Cracked
B6	5:30/165 PSI	—	—	—	—	—	60	Cracked
B7	5:30/165 PSI/ 600°C	-1.31	-9.87	-14.5	-3.77	65.0	60	
B8	6:30, vacuum	-6.85	-21.5	-48.2	-29.6	38.0	100	Smashed
B9	6:30, (N_2)	-1.66	-7.59	-11.9	-3.10	64.9	100	
B10	"	-1.97	-7.00	-17.7	-9.83	60.7	85	Glass cracked, pad bonded over
B11	"	-1.15	-5.09	-9.80	-3.89	66.3	96	
B13	"	-2.05	-7.64	-12.5	-3.32	66.8	75	
B14	"	-1.48	-5.00	-8.72	-2.21	68.0	70	
B16	"	-1.98	-3.28	-7.04	-1.94	66.0	99	Possible hairline crack
B15	5:45/165 PSI (620 600)	-4.85	-10.0	-25.7	-13.8	55.0	65	
B17	"	-2.01	-16.4	-19.3	-1.26	57.6	80	
B18	"	-1.80	-18.7	-22.3	-2.70	57.0	100	Cracked
B19	7:30/165 PSI/ 600°C	-1.19	-2.66	-10.1	6.79	62.0	100	
B20	"	-1.14	-1.31	-5.66	-3.32	68.3	100	
B21	"	-2.12	-5.56	-11.7	-3.75	68.0	100	
Average (uncracked cells)		-1.79 ±1.08	-6.47 ±4.18	-11.9 ±5.8	-4.02 ±3.42	64.6 ±4.3	85.4 ±15.4	

3.3.3 OCLI Production Cell Bonding

Three lots of one hundred cells have been purchased from OCLI for bonding process studies. The first of these was a lot of standard OCLI production cells, designated Production Lot 2092. These cells had relatively low, widely spaced metallization grid lines and a single-layer Ta_2O_5 AR coating. They were used to test the bonder parameters against a normal baseline cell, and to begin degradation studies. Table 15 gives the prebond characteristics of these cells. The following conditions were tested:

565°C, standard cycle

575°C, standard cycle

585°C, standard cycle

575°C, grooved electrode

570°C, new fixturing

560°C, new fixturing

570°C, 350°C preheat and new fixturing

The "new fixturing" tests checked a modified cell jig which holds the cell on top of the glass, as reported in Section 3.1.1; this jig is inverted from the original cell fixturing, which held the glass over the cell. Sample bond cycles are listed in Table 16. Tables 17 and 18 show the complete results of these bonds.

The cycle with preheat was shortened to 1 minute less than the cycle without preheat, to compensate for the faster temperature rise of the preheated cells. The temperature profile studies reported in Section 3.1.2 showed that the cycle with preheat brought cells to bonding temperature nearly 1 minute faster than a cycle without preheat.

Figures 10 and 11 show old fixturing bonds at 585° and 565°, while Figures 12 and 13 are typical before and after bonding I-V curves for, respectively, a 570° new fixture bond and a 570° new fixture bond with preheat and temperature offset. It is immediately noticeable that the bonds done at 570° without preheat showed less degradation than those done at 560° or done with the 350° preheat.

TABLE 15
CELL CHARACTERISTICS OF
OCLI PRODUCTION LOT 2092

Mechanical:

Size:	**2.00 cm x 2.00 cm**
Silicon:	**N/P**
Contact Line Height:	**2.1 μm $\pm$ 0.3**
Contact Line Width:	**150 μm**
Contact Spacing:	**3 lines/cm**
Surface Irregularity:	**~0.5 μm**
AR Coating:	**Single layer AR (SLAR)**

Electrical (Average):

V_{oc} (mV)	I_{sc} (mA)	P_m (mW)	CFF (%)
537.9	141.4	517	68.5
$\pm$9.5	$\pm$1.7	$\pm$70	$\pm$0.7

TABLE 16
SAMPLE BOND CYCLES, OCLI PRODUCTION LOT 2092

	Time	Pressure	Voltage	T_{top}	T_{bottom}	T_{Pre}
Baseline	0	0	0	565	565	20°C
Cycle	0:30	Contact	0			
	1:00	P↑	0			
	1:30	85	750			
	4:00	0	0			
New	0	0	0	570	570	20°C
Jigging	0:30	Contact	0			
	2:00	P↑	0			
	2:30	100	750			
	4:30	0	0			
Preheat	0	0	0	570	590	350°C
and Temp.	0:30	0	0		570	
Offset	1:00	P↑	0			
	1:30	100	750			
	3:30	0	0			300*

* Preheat power shut off at t = 0.
Actual table temperature measured at 300°C when sample was withdrawn onto loading table from bonding zone. Sample cooled from this temperature to 20°C.

TABLE 17
BONDING RESULTS FOR OCLI PRODUCTION CELLS, LOT 2092

Bond Temp. (C°)	Cell No.	% Bond	% Change in Electrical Properties				
			V_{oc}	I_{sc}	P_{max}	CFF	R_{se}
585	2	100	-1.5*	-5.0	-4.5	+1.4	0
	3	100	-2.4*	-2.7	-7.7*	-4.3	+ 25
	54**	80**	+0.9**	-21**	-44**	-22**	+170**
	55	80	+0.9	-1.4	-5.0	-4.6	+ 16
	Average	93	-1.0	-3.0	-5.7	-2.5	+13.7
575	4	95	+0.4*	-3.5	-4.3*	-1.4	-3
Ungrooved	7	90	+4.2*	-4.9	+10.6*	+11.0	-54
Electrode	52	100	+1.9	-2.8	-2.4	-1.4	-1.7
	53	100	0	+1.4	-1.7	-2.9	+50
	Average	96	+1.6	-2.5	-0.5	+1.3	-2.9
575	12	100	-0.6*	-0.7	-2.8*	-2.0	-75
Grooved	13	100	+0.1*	-1.8	-1.9*	-0.7	-76
Electrode	Average	100	-0.3	-1.3	-2.3	-1.4	-75
565	1**	80**	-1.2**	-30.3**	-42.3**	-14.7**	+107**
	14	95	-1.4*	-2.5	-2.0	-1.4	-79
	15	95	-2.2	-1.4	-8.3*	-3.7	-77
	42	95	-0.4	-0.5	+2.1	+3.0	-3.5
	Average	95	-1.3	-1.4	-2.7	-0.7	-53
Average** (12 cells)		95.8	-0.08	-2.15	-2.32	-0.6	-23
			±1.8	±1.8	±4.9	±4.3	±46

* Corrected for 17 mV V_{oc} error in prebond measurement.

** Cells 1 and 54 omitted from average due to grossly atypical performance.

TABLE 18
BONDING OF OCLI PRODUCTION CELLS WITH
NEW ALIGNMENT FIXTURE

Bond Temperature (°C)	Cell No.	% Bond	% Change in Electrical Properties				
			V_{oc}	I_{sc}	P_{max}	CFF	R
570	5	95	+0.6*	-2.5	-4.4*	-2.7	+17
	6	90	-4.5*	-1.4	-5.5*	+1.4	+98
	25	100	-0.4	+1.4	-1.8	-1.4	+98
	30	90	-1.7	-3.0	-6.2	-0.8	+1
	38	95	-0.9	-0.7	-3.8	-2.7	+15
	Average	94	-1.4	-1.2	-4.3	-1.2	+46
			±1.9	±1.7	±1.7	±1.7	±48
570	8	90	-1.1*	-2.2	-8.8*	-5.4	+24
with	11	95	-0.4*	-1.9	-8.2*	-6.2	+25
350	23	100	-1.8	-1.9	-10.6	-7.7	+60
preheat	48	98	+0.9	-1.4	-8.1	-7.6	+58
	Average	96	-0.6	-1.8	-8.9	-6.6	+42
			±1.2	±0.3	±1.2	±1.3	±20
560	9	95	-1.8*	-2.3	-8.7*	-1.8	-1.5
	10	95	-0.9*	-2.1	-9.5*	-5.1	+22
	19	100	+0.3	-1.4	-10.2	-8.8	+126
	37	100	0	-2.8	-5.7	-2.5	+16
	39	90	+0.9	-0.7	-0.8	-1.0	+16
	40	90	-0.4	-2.1	-5.6	-3.3	+25
	44	90	0	+1.4	-10.6	-11.5	+180
	Average	94	-0.3	-1.4	-7.3	-4.9	+55
			±.8	±1.4	±3.5	±3.9	±69

*Corrected for error in prebond measurement of V_{oc}.

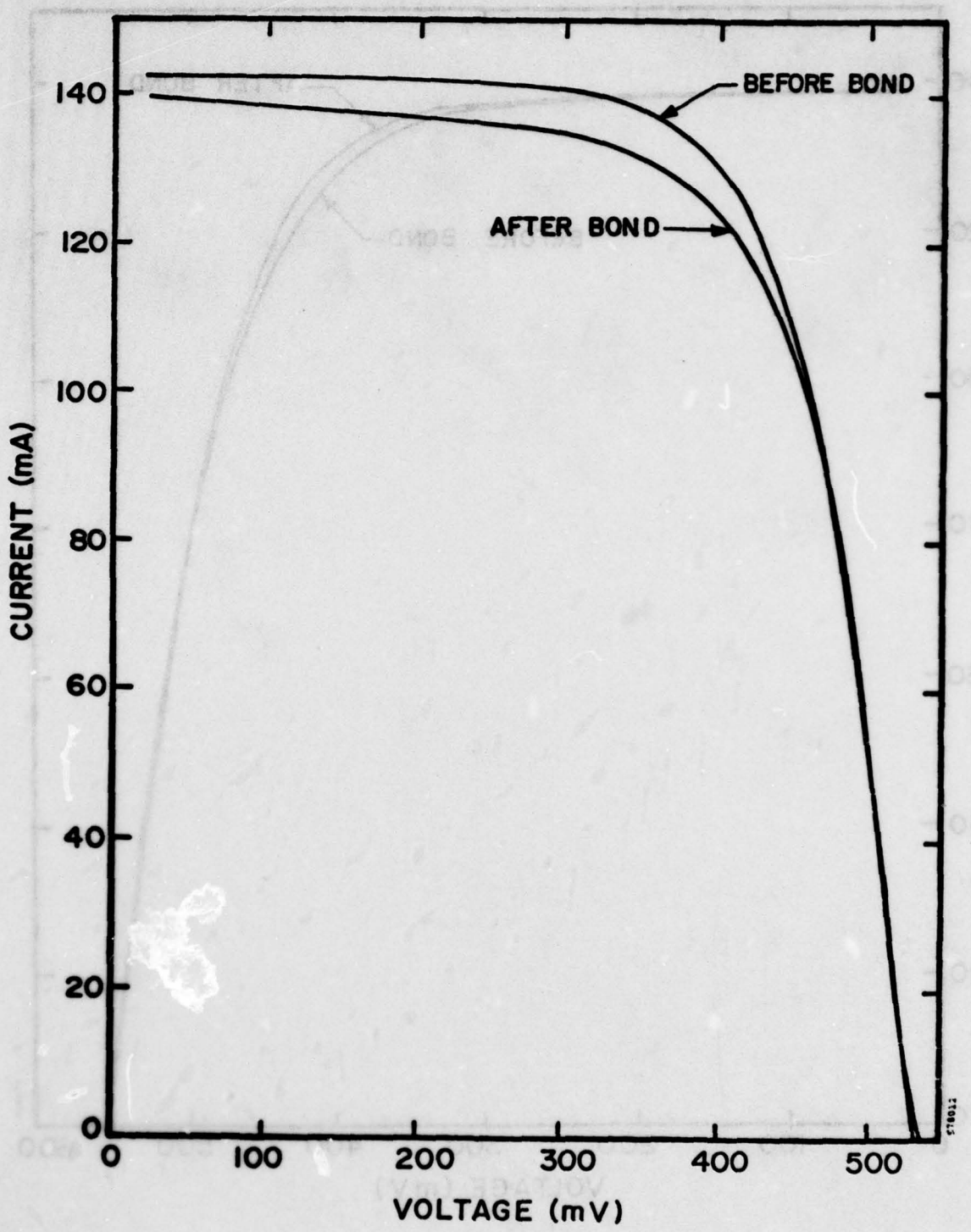

Figure 10. AM0 I-V Curve of OCLI Production Cell 2092-55 Before and After Bonding, Bonded at 580°C

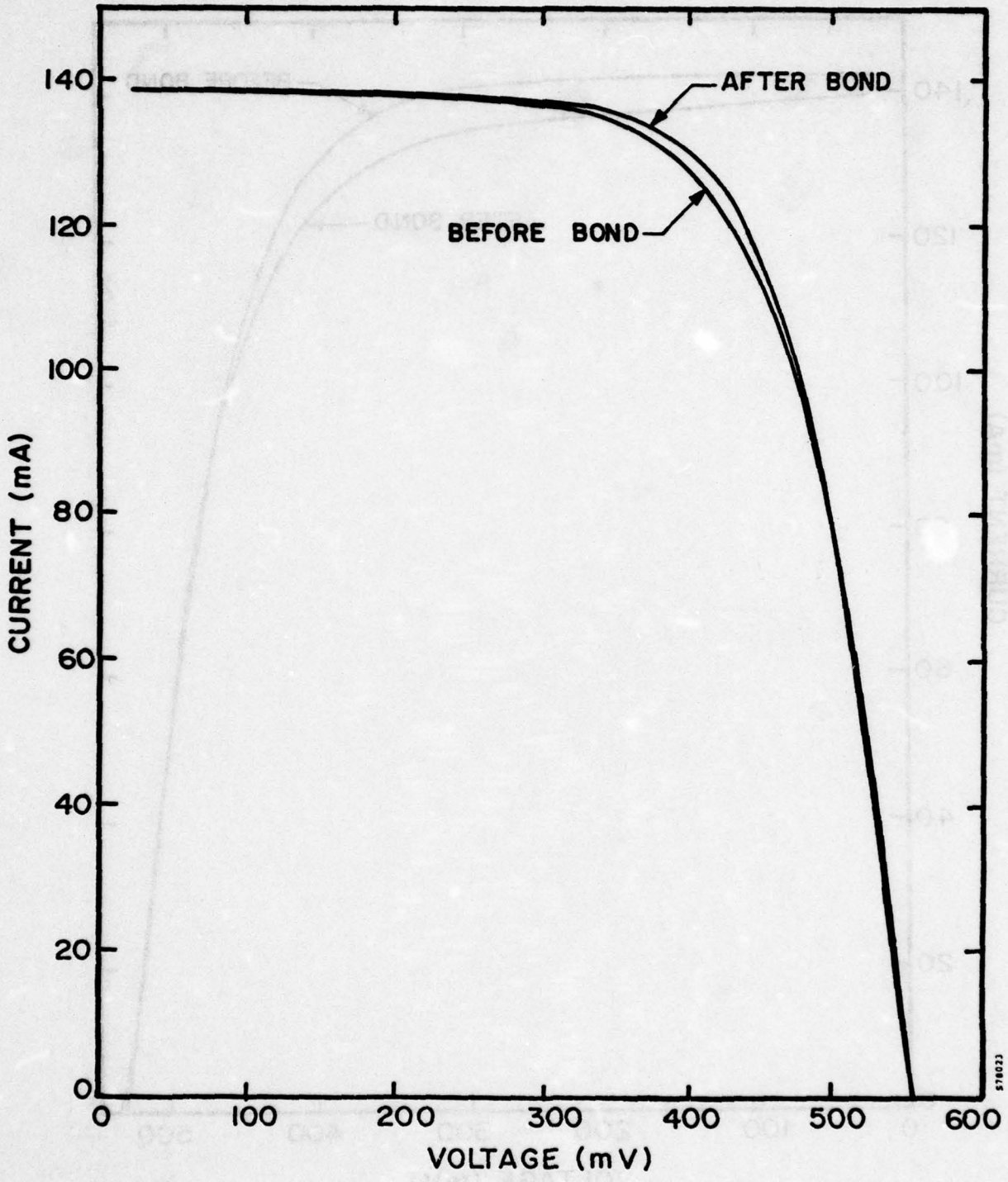

Figure 11. AM0 I-V Curves, Before and After Bonding, for OCLI Production Cell 2092-42, Bonded at 560°C

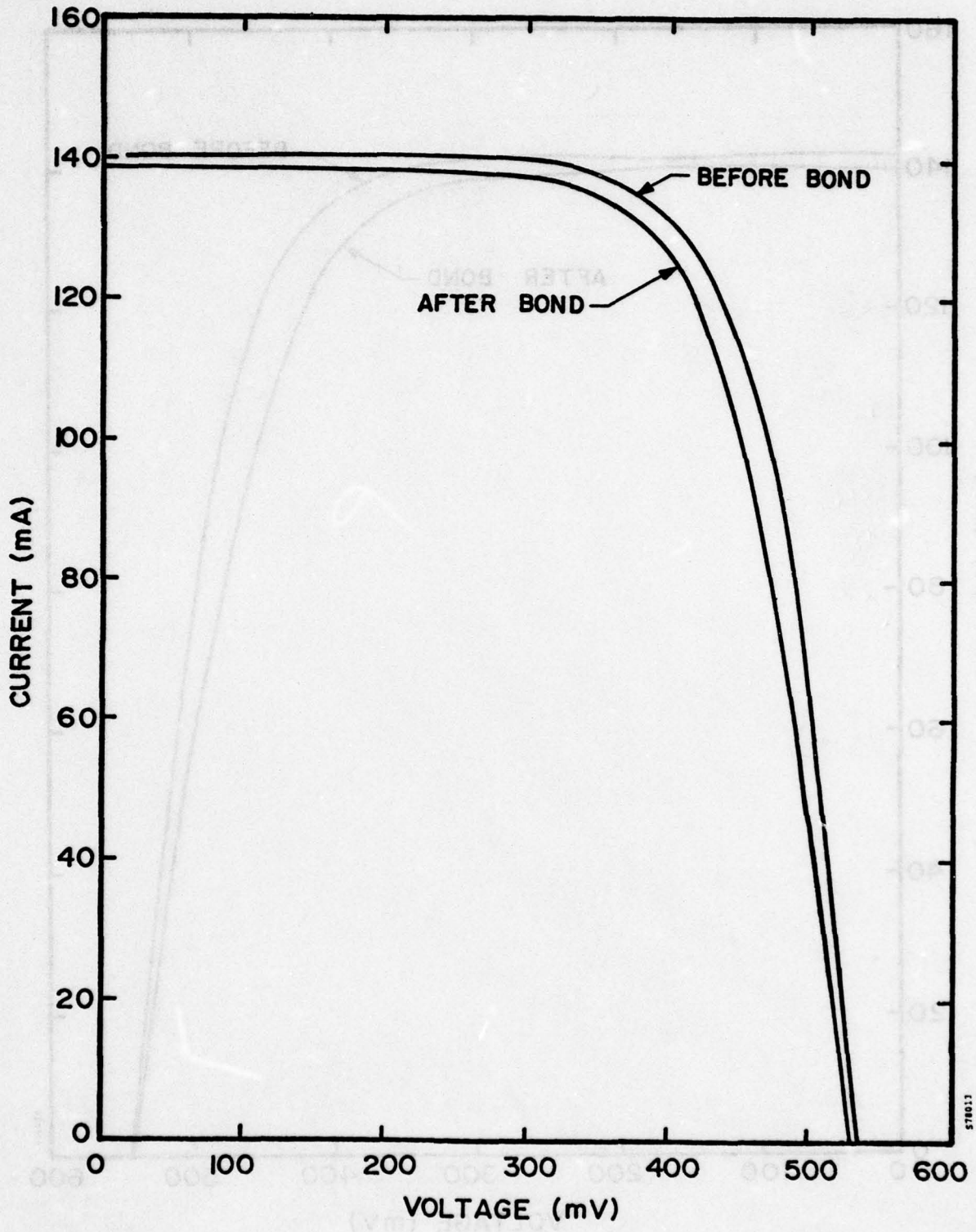

Figure 12. AM0 I-V Curves, Before and After Bonding at 570°C with New Alignment Jigging, for OCLI Production Cell 2092-38

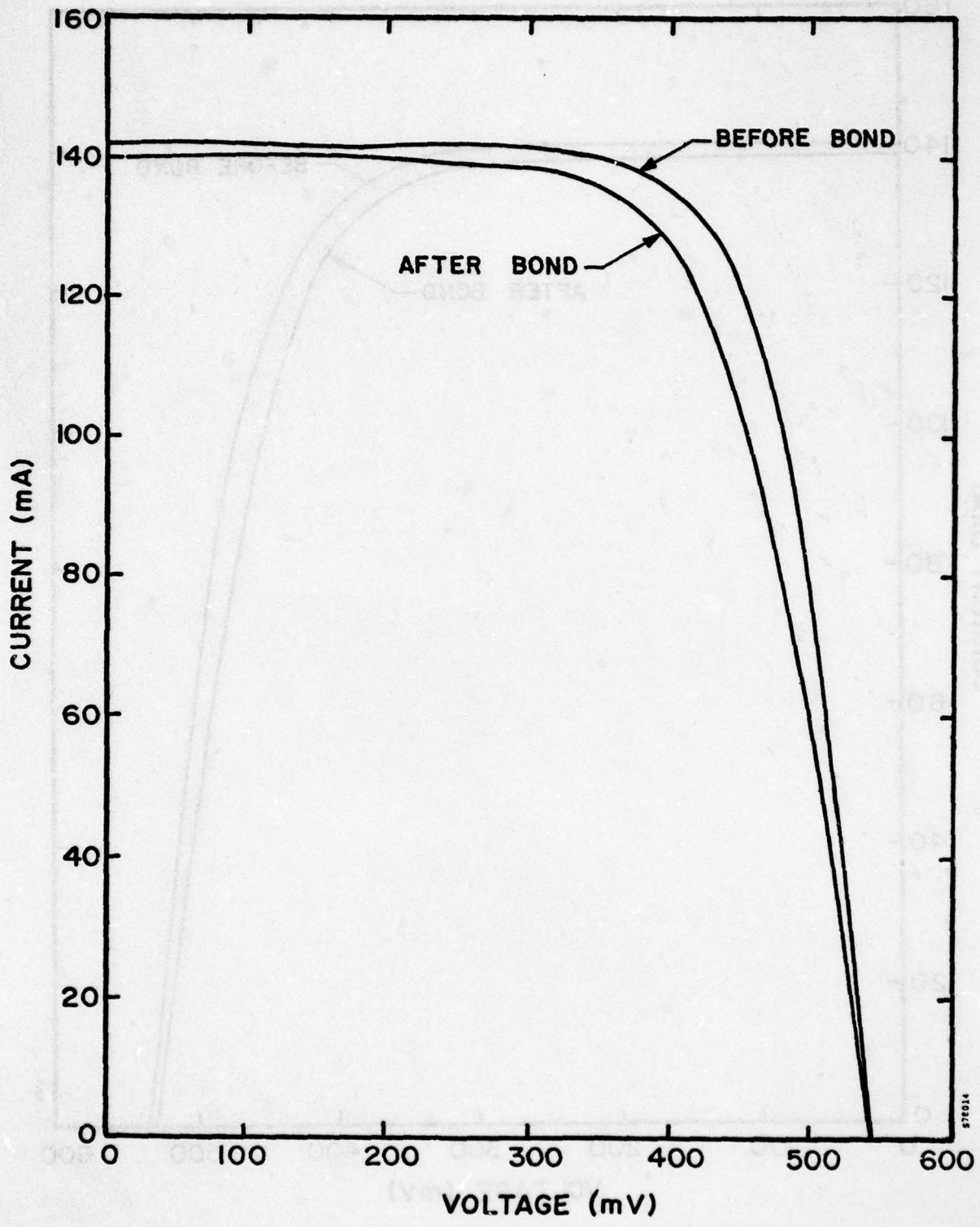

Figure 13. AM0 I-V Curves, Before and After Bonding at 570°C with 350°C Preheat and 20°C Bottom Heater Temperature Offset, for OCLI Production Cell 2092-48

An appropriate test for determining the statistical significance of the difference between the means of two sets of data is the "t" test. This test comprises calculating a t value, defined in Equation (1), and using statistical tables to establish confidence levels based on this t statistic and the associated number of degrees of freedom, which in this case is the total number of samples minus two.

$$t = \frac{\bar{Y}_2 - \bar{Y}_1}{S} \sqrt{\frac{n_1 \times n_2}{n_1 + n_2}} \qquad (1)$$

where $\bar{Y}_1, \bar{Y}_2$ are the means for the two sets of data in question,

S is the weighted RMS average of the standard deviations of each data set and,

n_1, n_2 are the number of samples in each data set.

Using this statistical test, we conclude from the given data on total power loss:

1. The 350° preheat cycle degrades cells significantly more in power than the corresponding cycle without preheat; valid with better than 99 percent confidence.

2. The 560° cycle tested degrades cells significantly more in peak power than the 570° bond cycle tested; valid with 89 percent confidence.

3. The difference between the degradation of P_{max} caused by the 570° bond cycle with new jigging, tested here, and that experienced by cells bonded with the old fixturing, reported last month, is not statistically significant. The apparent additional degradation of 2 percent shown by cells bonded in the new configuration is statistically confident with only 60 percent validity. In addition, the results on baseline bonding with the old fixturing are somewhat weighted by one cell (No. 2092-7) which showed dramatic improvement in power due to a very poor fill factor (62 percent) being corrected by sintering during the bond. Excluding this cell would make the two sets of results differ by only 0.8 percent. Thus, no definite conclusions about the relative merits of the two methods of alignment can be drawn, from these results.

It should be noted that although the new fixturing causes no noticeable improvement for these low efficiency cells, there may be a substantial improvement for higher efficiency cells with shallower junctions and correspondingly lower thermal tolerance. The results discussed in Section 3.4.4 indicate that thermal effects do not contribute significantly to the observed degradation of these cells. Thus the new jigging, which was designed to reduce thermal degradation, would not influence the bonding results, although it may help on higher efficiency cells.

The additional degradation of the cells bonded at 560°C may be due to the glass being excessively hard at the lower temperature, thus damaging the cells during the pressure cycle. The cause of degradation by the cycle with preheat is not clear. Possible explanations include thermal effects of the preheat or postheat, or effects of the temperature offset.

The second lot of cells, lot 83, purchased were 1-3 ohm-cm OCLI MLAR cells, with a 12.5 line/cm metallization pattern intended for high efficiency. The cells are slightly oversize. These cells are to be used for tests of bonded cell yield and degradation parameters. These tests have not yet been completed, however, initial tests have been done to determine bond parameters for these cells. Table 19 shows the results of bonds done on these cells to date. It is notable on these cells that good bonds with low degradation (3%) and high postbond power (66 mW) have been produced. Figure 14 shows the IV curve for a typical one of these cells.

A third lot of purchased cells, lot 2083, were 10 ohm-cm OCLI cells with an aluminum-alloy back-surface field (similar to lot 7C). They are also slightly oversize. These cells are intended for the tests of the effects of back-surface fields. Initial bond results on these cells are listed in Table 20. Although good bonding has been achieved on these cells, degradation remains at 12 percent, evenly divided between short circuit current loss and fill factor drop; leaving a postbond power of 63 mW for most of these cells. Appendix B contains the specifications for these two cell lots.

3.3.4 Degradation Studies

Further studies were done on production lot 2092 cells to isolate the cause of degradation during bonding. Two representative bond temperatures were chosen for tests, 570°C and 590°C. Cells were run through cycles at these two temperatures without applied voltage. Since a bond is not formed if no voltage is applied, these cells were tested without covers both before and after bonding.

TABLE 19
BOND RESULTS, OCLI 1-3 ohm-cm MLAR CELLS LOT 83

Cell	Cycle Variations	Percent Changes on Bonding V_{oc}	I_{sc}	P_{max}	CFF	Post-Bond Power (mW)	Bond %	Comments
1	600°C/6:30	-1.15	-1.33	-2.86	-0.26	67.8	100	
2	"	-0.00	-0.00	-0.00	-0.00	67.0	95	
3	"	0.17	0.68	-6.2	-4.9	64.7	80	
4	"	0.00	-6.9	-3.5	+3.5	64.3	80	
5	"	—	—	—	—	—	50	Output pad bonded, cell broken in removal
6	"	-0.04	-5.0	-35.9	-30.4	48.0	95	
7	600°C/7:00	-0.33	-0.00	-4.0	-3.5	67.6	95	
8	"	-0.50	-7.9	-24.4	-17.5	50.8	75	Cracked
10	"	-6.54	-71.2	-49.3	-81.1	32.6	100	Skewed, contact pad bonded, cell chipped in removal
AVERAGE*		-0.33	-1.78	-3.31	-1.03	66.3	90	
		±0.48	±2.91	±2.24	±3.3	±1.7	±9.3	

*Excluding cells 5, 6, 8, and 10

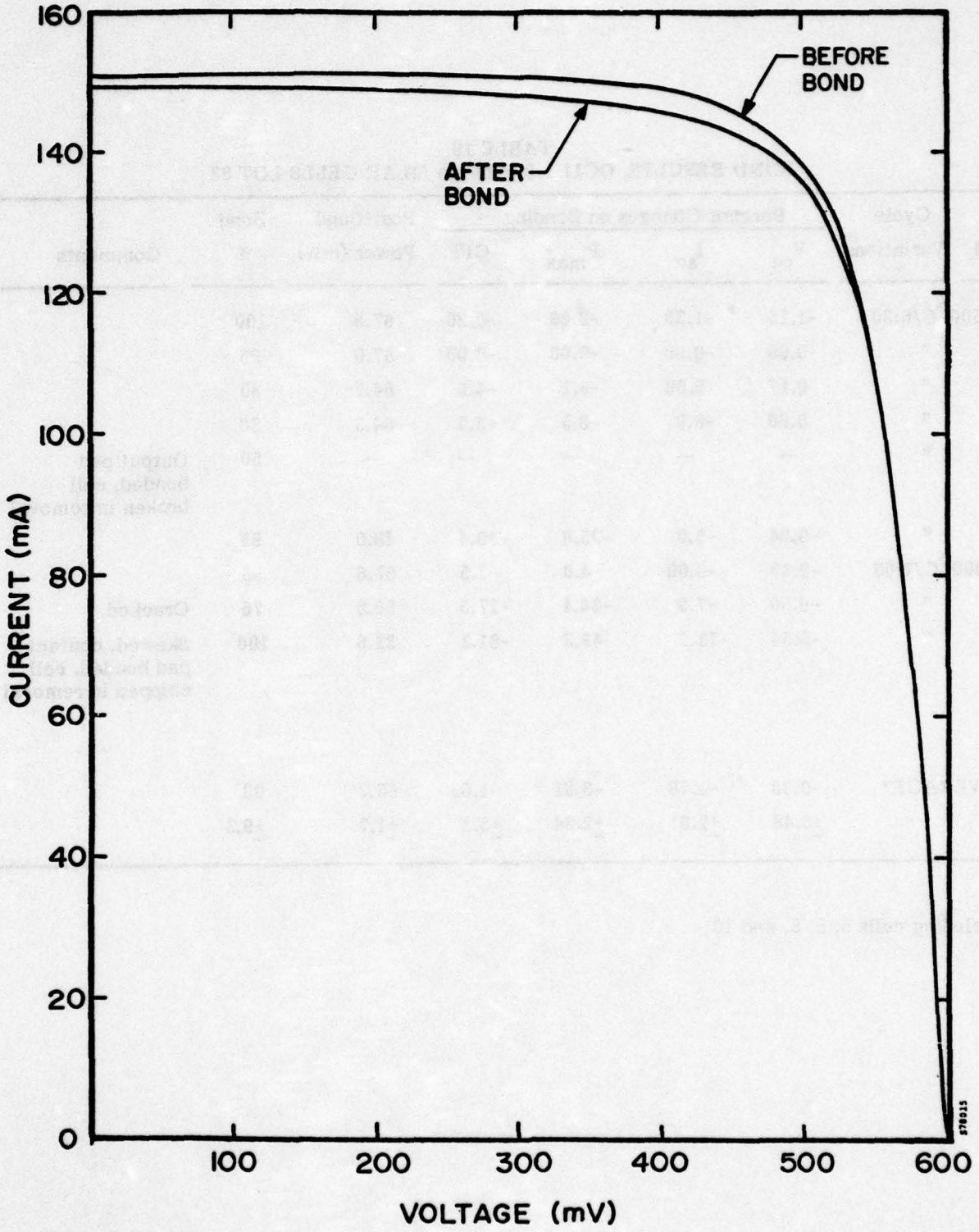

Figure 14. Before and After Bond I-V Curve for Cell 83-1

TABLE 20
BOND RESULTS, OCLI 10 ohm-cm MLAR CELLS LOT 2083

Cell	Percent Change						
	V_{oc}	I_{sc}	Pm	CFF	P_{max}	% Bond	Comments
1	-12.9	-62.5	-76.8	-30.8	16.0	70	Short in bonder
2	-2.6	-3.7	-15.0	-8.9	60.3	85	
3	-1.0	-9.0	-13.7	-4.1	63.0	98	
4	-	-	-	-	-	20	Sample slid, contact pad bonded
5	-0.9	-3.2	-6.9	-3.1	63.0	95	
6	-2.7	-7.3	-17.7	-8.8	62.1	90	
7	-0.7	-5.5	-7.2	-1.2	70.0	98	
Ave*	-1.6 $\pm$1.0	-5.7 $\pm$2.5	-12.1 $\pm$4.8	-5.2 $\pm$3.5	63.7 $\pm$3.7	93.2 $\pm$5.6	

*Does not include cells 1 and 4

Three cells were run at each combination of time/temperature. Except for the first set of bonds, which were run as a control with only contact pressure, all of the bonds for the experiment were run at 100 PSI bond pressure. Thus, the combined effects of temperature and pressure were studied separately from the effects of voltage and cover glass optical coupling. The test mainly studied the 570°C bond, which was the standard bond cycle at that time.

In general, for short duration bond cycles, there is an increase in cell power after the degradation test. This is due to an improved curve fill factor after the heat cycle, presumably as an effect of additional sintering of the cell contacts. At 570°C, cycle times of over 10 minutes were needed before thermal degradation became greater than this incidental improvement. Results for durations up to 6 1/2 minutes are shown in Table 21. Complete results are listed in Appendix C. Figure 15 shows the test results plotted as power loss in percent versus time in bonder in minutes, for two temperatures. For clarity, data points within $\pm$30 seconds of 5 minutes have been averaged on the graph, although they were taken separately for linear regression calculations. Degradation appears to be linear with bond cycle duration. The least-squares fit to the data is plotted. From these data, the power loss due to temperature and pressure alone is calculated to be -0.43 percent per minute at 570°C, and -2.69 percent per minute at 590°C. The correlation coefficient (a measure of how well the data fit the linear approximation) is -0.70 for the 570°C data and -0.86 for the 590°C data, indicating good correlation. There was no significant difference in degradation between tests with contact pressure only and tests with 100 PSI pressure.

This apparent lack of degradation of the cells exposed to bond temperature and pressure leaves two major possibilities for the cause of degradation:

1. Degradation associated with the glass cover.
2. Degradation due to applied voltage.

Degradation due to the glass cover could be contamination on the glass induced during bond, changes in glass composition, or a glass/cell interaction. Most of these effects reduce incident light intensity and thus would be expected to affect short circuit current only. To look for this effect, the unbonded coverglasses from four of these degradation test cells were optically coupled to an unbonded cell using isopropyl alcohol. Since isopropyl alcohol has an index of refraction very close to that of 7070 glass, this configuration should perform optically like a bonded cell. These covers had been through

TABLE 21
PRESSURE PLUS TEMPERATURE DEGRADATION
FOR OCLI LOT 2092 CELLS

Percent Change from Prebond Measurements

No Voltage Applied
(All Measurements Done Without Coverglass)

Bond Duration (min)	Cell No.	V_{oc}	I_{sc}	P_{max}	CFF	R_{SE}
4 1/2	16	-0.2	-0.2	-1.3	-0.6	+20
Contact Pressure	17	+0.4	+0.9	+6.0	+7.0	-29
Only	18	-0.1	-0.5	-1.9	-2.9	+9.4
	Avg.	0	+0.1	+0.9	+1.2	0
4 1/2	21	-1.3	0	+0.6	+4.0	-8.7
	22	-3.1	-1.0	+8.5	+14.5	-50
	24	-3.0	0	-3.3	-0.6	+0.7
	Avg.	-2.4	-0.3	+1.9	+6.0	-19
5	26	-3.2	-0.3	+11.0	+16.0	-40
	27	+0.2	+1.1	+1.9	-0.2	+11
	28	-1.6	+3.2	+13.0	+13.3	-32
	Avg.	-1.5	+1.3	+8.6	+9.7	-20
5 1/2	31	-1.2	+2.1	-4.0	+6.0	-8.7
	32	+1.0	0	+3.5	+3.0	-5.0
	33	0	+0.7	-5.6	-6.2	+31
	Avg.	-0.4	+0.9	-2.0	-0.9	5.8
6 1/2	34	+0.9	-0.7	-1.5	-1.9	+25
	35	+0.7	+0.7	+6.7	+6.0	-15
	36	-0.7	0	+0.2	-5.5	+6.2
	Avg.	+0.3	0	+1.8	-0.5	+5.4
Average of all 18 cells		-0.6 (±1.4)	+0.6 (±1.2)	+2.4 (±5.3)	+3.2 (±6.5)	-5.1 (±23.6)

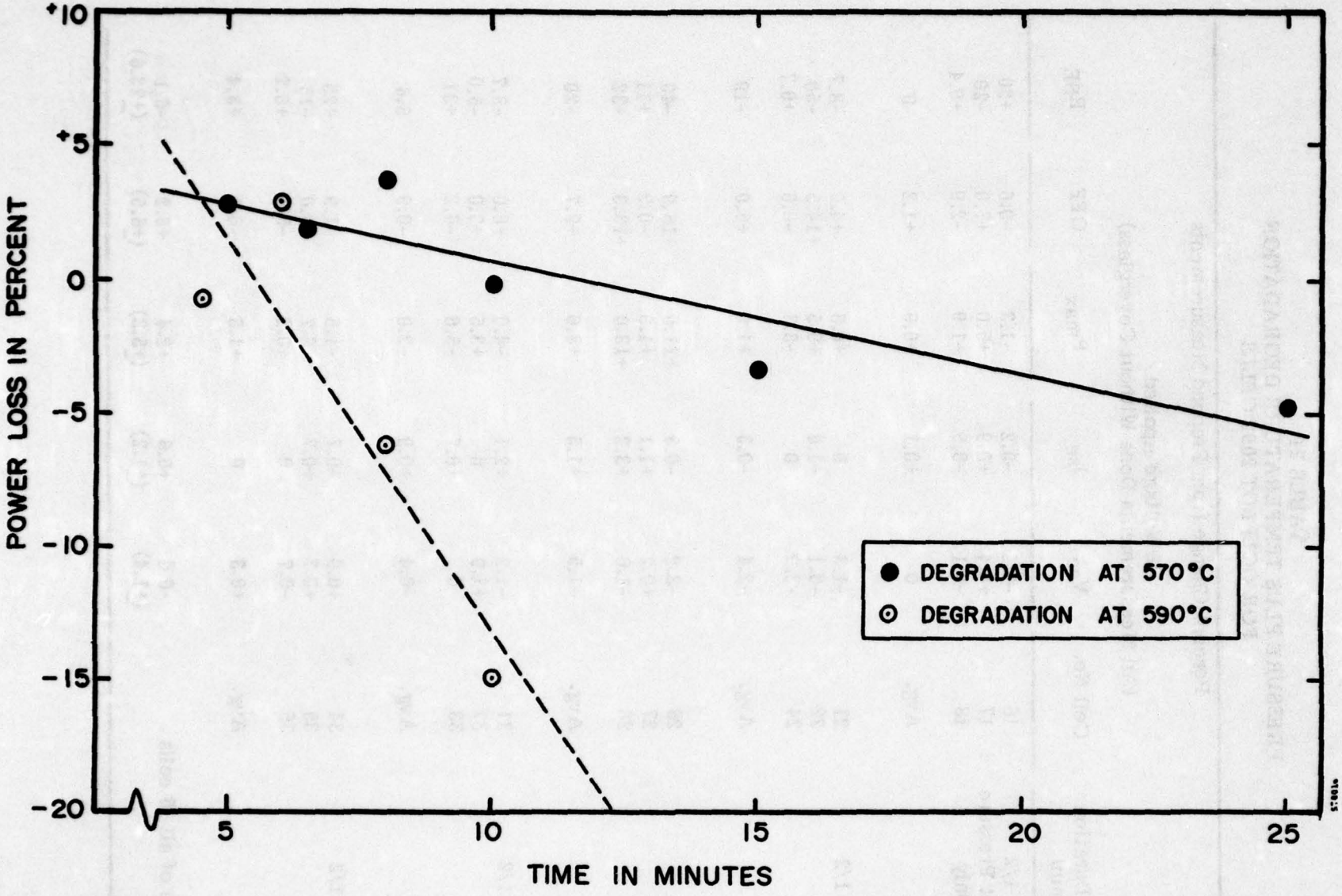

Figure 15. Power Loss Plotted Against Bond Duration at Zero Applied Voltage for Two Different Temperatures for OCLI Lot 2092 Production Cells

the bonding heat and pressure cycles, and thus would be expected to show any degradation caused by this aspect of the bond. Results of the measurements from the cell with fresh (not previously bonded) and old (previously bonded) coverglasses, attached the same way, and for the cell without cover were compared. Average values of I_{sc}, taken on the same cell with different covers, are listed below:

Bare cell:	I_{sc} = 138.5 mA
Cell with fresh cover:	I_{sc} = 139.7 mA
Cell with previously bonded cover:	I_{sc} = 139.0 mA

From this comparison we conclude that, while there may be some small optical losses in the cover due to the heat/pressure cycle, they are not enough to cause significant power loss.

To eliminate the possibility that the high voltage, acting in combination with pressure and temperature, puts contaminants into the glass by field-assisted diffusion, electrochemical ion exchange, or other mechanisms, the short circuit current of five bonded cells from lot 2092 were measured before and after the covers were ground on a diamond wheel to remove the outermost layer of glass, and with it any contaminants in that layer. The results are shown in Table 22. These results correspond to plus or minus one unit in the least significant digit. We can thus conclude that contamination introduced into the surface of the coverglass is not the source of short circuit losses in these cells.

There are several possible mechanisms for voltage induced cell degradation, including voltage induced cracking, damage caused by the electrostatic forces on the cell, electromigration of ions into the silicon and arcing, either through the glass cover, around the edges of the cover, or across a residual cell/glass gap due to a too early application of voltage. It should also be noted that the apparent absence of purely temperature-dependent degradation at short bond durations for these low efficiency cells does not rule out the possibility that higher efficiency cells may experience significant amounts of degradation due to temperature.

TABLE 22
SHORT CIRCUIT CURRENT BEFORE AND AFTER
COVER GLASS ABRASION (OCLI LOT 2092)

Cell	I_{sc} (Before Grinding) (mA)	I_{sc} (After Grinding) (mA)
6	143	142
7	137	138
10	140	141
13	139	140
52*	144*	143*
Average difference after grinding = + 0.36%		

* Cell 52 drastically lost fill factor. Since on this cell the abrasion may have extended through the glass cover to the cell surface, this data point was discarded.

OCLI lot 2092 production cells were used in an attempt to quantify the effect of voltage dependent degradation. Bond cycles used are listed in Table 23. These cycles were designed to hold constant both the total time at temperature and the product of voltage with bond time. Results are shown in Table 24. Increased degradation was seen for the lower voltage bond; however, the difference between the two cycles is not seen to be statistically significant by the t test. Both bonds showed more degradation than predicted by the thermal-cycle-only test results reported above. Additional experiments are being done to quantify the voltage dependent behavior and to investigate the effects of voltage turn-on rate.

The method in which voltage is first applied may have an effect on cell degradation. Application of high voltage before silicon/glass interface is closed may cause arcing which damages the cell. When voltage is first applied to a sample, current begins to flow only through those points at which glass and silicon are in contact. Since the glass composition is initially uniform, the flow is primarily directly to the electrode, leaving the region adjacent to the contact point largely unaffected. The small gap between the materials then supports virtually the entire applied voltage. The resulting electric field draws the surfaces into intimate contact so that bonding can occur, but if the voltage is too high, it may also cause arcing, damaging the cell surface.

TABLE 23
BOND CYCLE FOR VOLTAGE DEPENDENCE DEGRADATION EXPERIMENT

	Time (min:sec)	Pressure (PSI)	Voltage (V)	T_{top} (°C)	T_{bot} (°C)
(A) high voltage short duration	0	0	0	570	590
	0:30	Contact	0	570	570
	1:30	P↑	0	570	570
	2:00	100	800	570	570
	4:15	100	0	570	570
	8:00	0	0	sample withdrawn	
(B) low voltage long duration	0	0	0	570	590
	0:30	Contact	0	570	570
	1:30	P↑	0	570	570
	2:00	100	300	570	570
	8:00	0	0	sample withdrawn	

TABLE 24
DEGRADATION DEPENDENCE ON VOLTAGE,
OCLI LOT 2092 CELLS

		Bond Results (% Change)				
Cycle	Cell	V_{oc}	I_{sc}	P_m	CFF	Bond %
A	73	-1.48	+1.44	+4.20	+3.33	87
	74	-0.55	-3.47	-6.63	-2.21	88
	78	0	-1.42	-2.73	-0.97	90
	Ave.	-0.68±0.78	-1.15±2.47	-1.72±5.48	+0.05±2.91	88
B	79	0	-2.14	-2.20	-4.21	90
	85	-0.93	-3.57	-6.00	-1.93	90
	90	-1.49	-5.07	-5.18	+1.01	70
	Ave.	-0.81±0.75	-3.59±1.47	-4.46±1.96	-1.71±2.62	83

Such microarcing could account in part for the possible dependence of cell degradation on the application of voltage. It may be that damage is due less to the voltage level involved than to its abrupt application. A high voltage might be supported without arcing if the sample were first exposed to a low voltage for a time. During this period, the glass around the point of contact is depleted of mobile ions, and becomes much more resistive than the bulk of the glass. A large fraction of the current can then be expected to follow low resistance paths outward from the contact point, around the depleted region, reducing the voltage across the gap near the contact point, and increasing the voltage that the sample can support without arcing.

This analysis suggests that it may be desirable to raise the voltage to its maximum value slowly, rather than applying the full voltage instantaneously. A series of experiments is planned to test this hypothesis. Cells will be bonded under conditions in which the maximum voltage and total charge transfer are held constant, while the rate at which the voltage is increased is varied.

For the component of degradation purely due to temperature, we expect an exponential dependence of degradation on temperature. The results reported show an increased degradation rate by a factor of 2.5 for every 10°C increase in temperature. In comparison, the viscosity of 7070 glass decreases by approximately a factor of 1.8 for every 10°C increase in temperature.[6] This confirms the policy of bonding at the minimum usable bond temperature. Our studies indicate that degradation due to excessively hard glass starts for bonds at 560°C or below. Longer bond cycles with lower pressure may alleviate this problem.

If the thermal degradation is in fact due to diffusion-related effects, we expect the thermal degradation rate R to be

$$R = C\, e^{-\frac{x_j}{x_o}}\, e^{\frac{kT}{E_a}}$$

where C is an arbitrary constant (dependent on severity of degradation and units of measurement)

x_j is junction depth

x_o is a characteristic depth, dependent on impurity diffusion length

k is Boltzmann's Constant ($8.62\ 10^{-5}$ eV/^oK)

T is temperature

E_a is a characteristic energy of degradation (dependent on mechanism)

In general, there may be several degradation mechanisms, causing the total degradation to be a sum of such terms. It is noted that thermal degradation is expected to be exponentially decreasing with junction depth. This dependence will be confirmed in tests on OCLI lot 2083 cells.

3.4 METALLIZATION VARIATIONS

3.4.1 Molybdenum-Silver Metallization

Iles and Faith, as a result of their investigations of thermal degradation rates for different contact metals, found a molybdenum-silver system to be among the most resistant to thermal degradation.[7] Scott-Monck et al. also found molybdenum to be a good high temperature barrier.[8]

An experimental lot of ten 2 x 2 cm cells with molybdenum-silver contacts has been produced and bonded at Spire. Ninety-five percent bond coverage with improved electrical performance has been demonstrated. These cells were made from 10 ohm-cm material with implanted BSF. Contact metallization consisting of 400A of molybdenum, followed by 2 μm of silver, was applied entirely by evaporation. Even without sintering, the cell series resistance averaged 0.044 ohm for the lot, and in six cases was below the limits of our measuring sensitivity. Average characteristics of the lot are given below:

V_{oc}: 578.2 mV

I_{sc}: 135.4 mA

P_{max}: 60.3 mW

CFF: 77.7%

Metallization thickness: 2.3 μm

Five of the cells showed bond coverage exceeding 90 percent. Two were bonded in a 5-minute cycle at 620°C and 200 PSI and emerged badly broken. Another, bonded at 600°C and 150 PSI, showed severe electrical degradation of unknown origin. The remaining two, cells 2 and 4, were bonded at 580°C and 200 PSI, and showed little or no degradation. The pre- and postbond I-V curves of the best cell, No. 2, showing an increase of 2.7 percent in maximum power, are shown in Figure 16. The bond cycle used with these cells is shown in Table 25 and complete bond results are listed in Table 26. Of particular interest is cell 5, which showed very little degradation, even after 5 minutes at 610°C, demonstrating the thermal stability of the MoAg combination.

3.4.2 Summary of Metallization Systems Bonded

One of the goals of this program is to study the effect on bondability and degradation of cells caused by variations in cell process parameters, including various cell materials, contact materials, and junction depths. Since this baseline has not been established until late in the investigation, it is appropriate to see what information on the effect of the contact metallization has been learned from the experiments already conducted. As metallization variations have been concurrent with variations in contact height and spacing, cell material, junction depth, and other parameters, any conclusions must be considered tentative.

In all, six metallization systems have been tried: silver (OCLI lot 3C), palladium-silver (OCLI 3A, 3B), vanadium-silver (OCLI 7A), molybdenum-silver (Spire lot 1633), titanium-silver (OCLI 4a, 8, 9), and titanium-palladium-silver (OCLI 4b, 4c, 4d, 4e, 5B, 6, 7B, 7C, 10, 11). A summary of the results is presented in Table 27. Of those cells of each metallization type having bond coverage of at least 80 percent, the half showing the least degradation in maximum power were selected for inclusion in the data of Table 27. Metallization heights, and accordingly bonding conditions required to accommodate them, varied among the results.

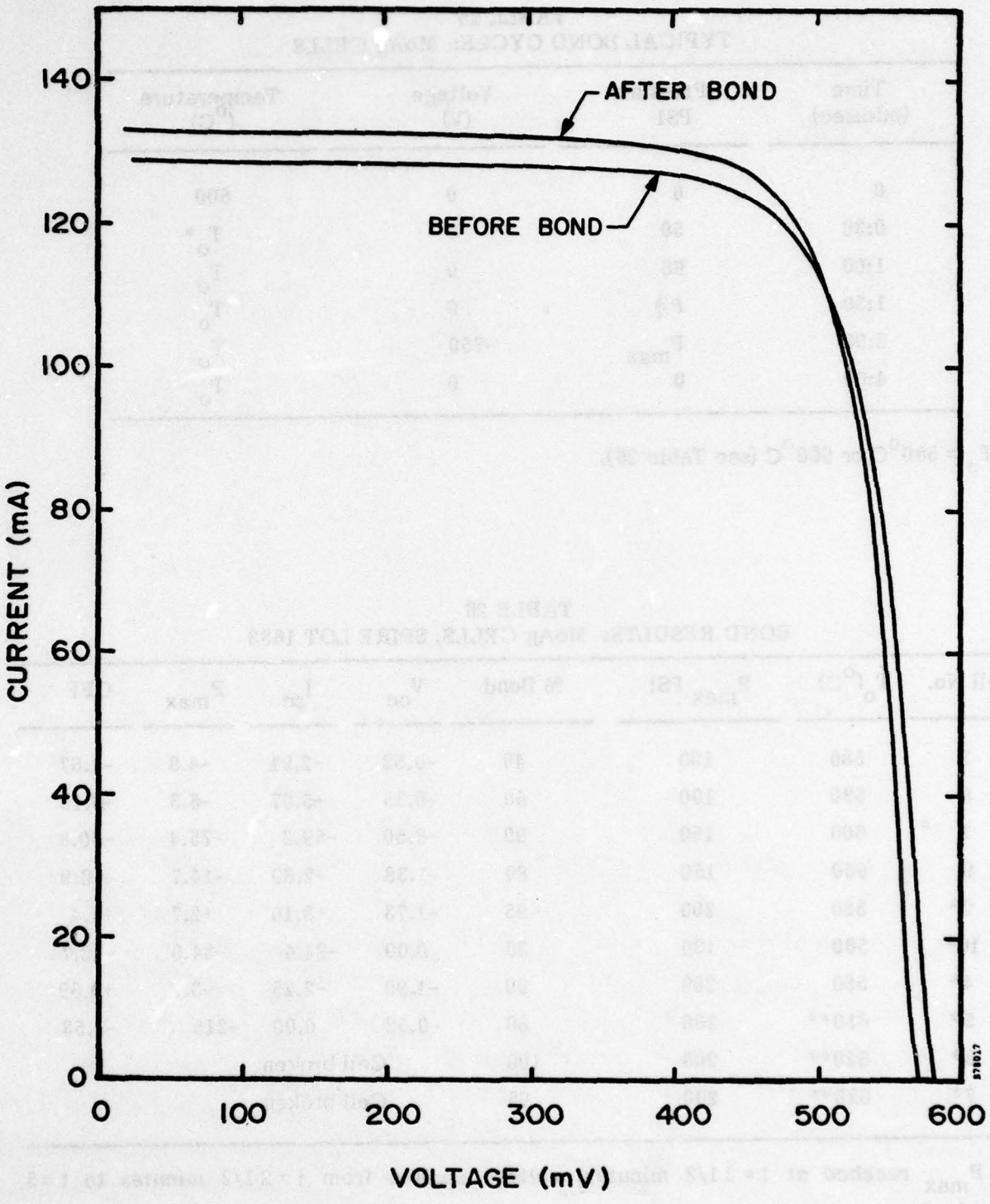

Figure 16. Before and After Bonding I-V Curves for Molybdenum-Silver Metallization Cell 1633-2

TABLE 25
TYPICAL BOND CYCLE: MoAg CELLS

Time (min:sec)	Pressure PSI	Voltage (V)	Temperature (^{o}C)
0	0	0	600
0:30	50	0	T_o*
1:00	60	0	T_o
1:30	P↑	0	T_o
2:00	P_{max}	-750	T_o
4:00	0	0	T_o

* T_o = 580^{o}C or 600^{o}C (see Table 26).

TABLE 26
BOND RESULTS: MoAg CELLS, SPIRE LOT 1633

Cell No.	T_o(^{o}C)	P_{max} PSI	% Bond	V_{oc}	I_{sc}	P_{max}	CFF
3	580	100	40	-0.52	-2.91	-4.9	-1.67
6	580	100	60	-0.35	-5.67	-6.3	-0.13
1	600	150	99	-8.50	-59.2	-75.4	-30.8
9	600	150	80	-1.38	-2.89	-14.7	-10.9
2*	580	200	95	-1.73	+3.10	+2.7	+1.4
10*	580	100	30	0.00	-24.4	-34.0	-12.7
4*	580	200	90	-1.90	-2.25	-3.7	+0.39
5*	610**	200	80	-0.52	0.00	-215	-1.53
8*	620**	200	100	Cell broken			
7*	620**	200	95	Cell broken			

* P_{max} reached at t = 2 1/2 minutes; voltage applied from t = 2 1/2 minutes to t = 5 minutes.

** Temperature constant at this value throughout bond.

TABLE 27
BOND RESULTS FOR CELLS WITH SIX DIFFERENT TYPES OF METALLIZATION

Contact Material	No. of Cells	Cell Lots Included	Average Bond Coverage (%)	Average Postbond Power (mW)	Average Percent Change V_{oc}	Average Percent Change I_{sc}	Average Percent Change P_{max}	Average Percent Change CFF
Ag	1	3C	100	40	-2	+18	-15	-25
VAg	1	7A	90	27.1	-9.8	+7.0	-40.3	-38.2
PdAg	3	3A, 3B	100	41.3	-0.33	+18.7	-1.00	-14.7
MoAg	3	1633	88.3	58.4	-1.38	+0.28	-1.04	+0.09
TiAg	11	4A, 8	92.7	60.8	-0.28	-1.47	-6.32	-4.40
TiPdAg	17	4B,C,D,E 5B,10 11A,B	89.9	57.5	-0.44	-0.44	-4.28	-3.40

Note: Lot 1633 (MoAg) produced at Spire, remainder were OCLI cells.

Although the small amount of data available compels caution in drawing conclusions, it appears that silver, vanadium-silver, and palladium-silver contacts are highly susceptible to high temperature degradation. The small power loss of the PdAg cells includes a large fill factor loss. The post-bond power is still very low.

Our positive results with molybdenum-silver contacts are in good agreement with the conclusions of Iles and Faith regarding these materials. Surprisingly, while Iles and Faith found titanium-palladium-silver to be substantially inferior to titanium-silver in thermal stability, our results indicate that the three-metal-system is at least equal, if not superior, to titanium-silver in this regard. The source of the discrepancy may be the "mesa" contact structure used in the experiments of Iles and Faith, in which only the barrier metal is in contact with silicon. Only the most recent lots from OCLI have used this structure, so that most of the data in Table 27 are from cells with standard contact patterns, the silver overlapping the barrier metal(s). If, as Iles and Faith found, the primary source of thermal degradation in TiAg-contacted cells is the TiAgSi interface, the presence of this interface in both TiAg and TiPdAg standard contacts could account for the similarity of the results.

3.5 HESP CELL BONDING

Experiments have been begun to demonstrate the bonding of texture etched silicon, such as that used to reduce surface reflection on some high efficiency solar cells, including the HESP cells (Air Force Contract F33615-75-C-2028). Sample textured silicon was produced by hydrazine etch at Spire Corporation. Four samples of this material have been bonded at 600°C. An 8-minute bond, using a maximum pressure of 140 PSI (corresponding roughly to the pressure usually applied to spacecraft cells), resulted in bonding only of the peaks of the surface tetrahedra, which were left imbedded in the glass when the sample was broken off. Slight improvement was achieved by increasing the peak pressure, but cracking of the silicon became a problem at 250 PSI. However, a good, though still incomplete, bond has been achieved, using a 12-minute cycle and 200 PSI pressure. These bonds are visually acceptable and mechanically strong. Further lengthening of the cycle, coupled with higher bond voltages, may permit complete deformation and bonding of the textured surface.

Figure 17a shows the surface of the textured silicon used in these experiments. Texturization height was on the order of 15 micrometers. Finer structure may permit easier bonding and will be tried in later tests. Figure 17b shows a finer structure in the same scale as Figure 17a.

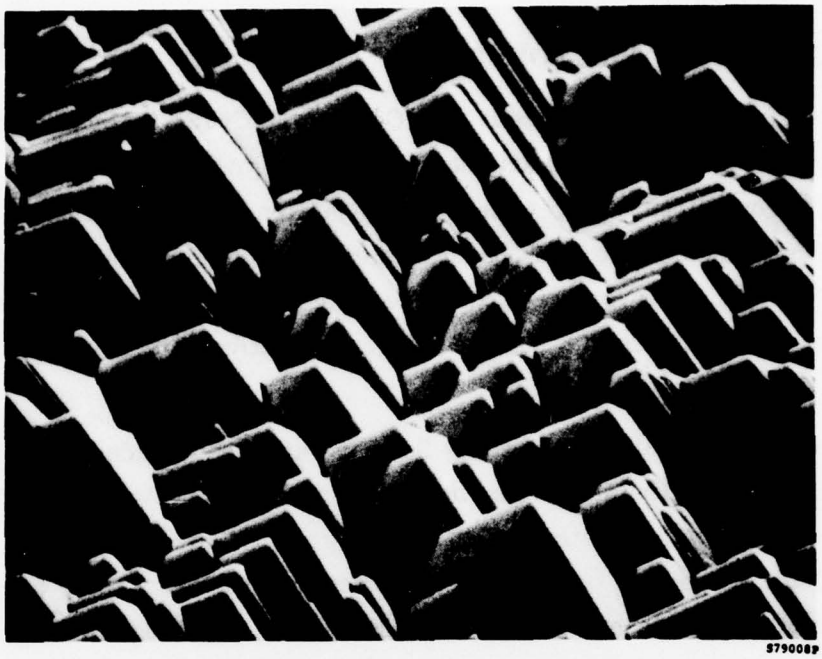

(a)

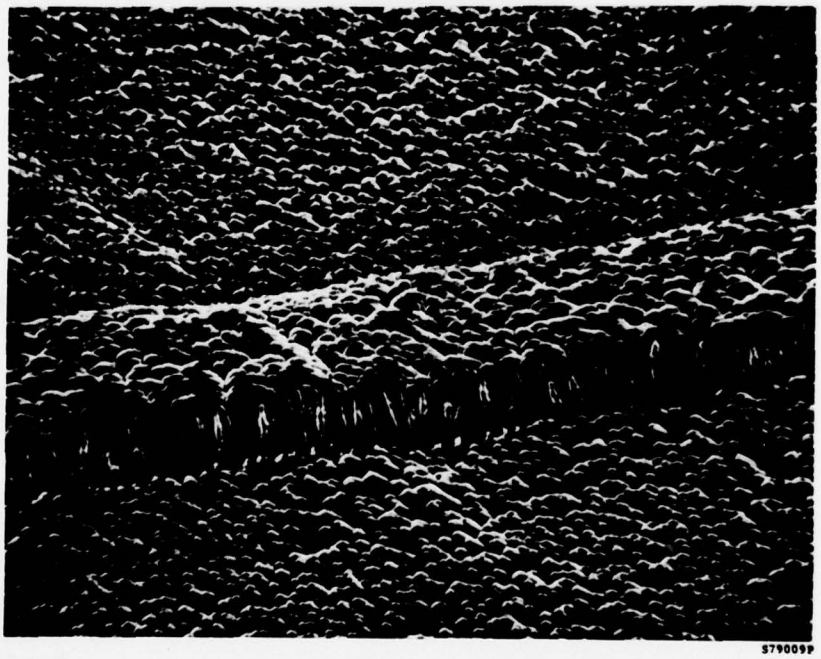

(b)

Figure 17. Scanning Electron Micrographs (1000X) of (a) Spire Texturized Silicon, Produced by Hydrazine Etch, and (b) HESP Cell Surface, Texturized by NaOH/Alcohol Etch

3.6 VERTICAL JUNCTION CELL BONDING

Nonreflective vertical junction cells (AF Contract F33615-76-C-2058) produced by etching deep grooves on (110) silicon have shown significantly greater radiation resistance than planar silicon cells, with a potential for high efficiency.[9] Ordinary adhesively bonded covers for these cells have a potential problem of breaking the fragile cell walls during the expansion/contraction cycles encountered in solar eclipse periods. This problem may be alleviated by the use of electrostatically bonded cover glasses, which are a close thermal match to silicon.

Ten vertical junction cells produced by Solarex have been bonded. Finding a bond cycle which avoids cracking the silicon has been difficult. Bond coverage is low, mostly due to the high (9-μm) metallization. Bonding is good in the areas away from the metallization, and the completed bonds withstand thermal cycling. A long bond cycle — 10 minutes — must be used to achieve good bonds without cracking the cell. Table 28 shows pre- and postbond cell results.

TABLE 28
BOND RESULTS, VERTICAL JUNCTION CELLS

Cell	Change from Prebond Parameters V_{oc}	I_{sc}	P_{max}	CFF	Post-bond Power (mW)	% Bond	Comments
1	-0.56	-4.2	-7.5	-2.8	53.3	25	Glass cracked
2	-4.4	-6.8	-24.1	-15.5	44.0	65	Cell hairline fracture
7	-4.0	-2.6	-22.0	-16.1	47.2	83	
8	-9.3	-7.4	-39.3	-27.0	35.8	30	Many hairline fractures
13	-2.0	-8.8	-16.1	-6.4	47.0	35	
14B		-	-	-	-	-	Cell broken
15	-5.6	-12.2	-30.4	-16.1	40.7	95	Cell broken
17	-	-	-	-	-	12	Cracked, contact pad bonded over
19	-2.7	-9.7	-11.0	+1.3	50.2	30	Cell cracked

Note: Cells 1, 2, 8 and 19 bonded at 590 → 575°C, 4 minutes, varied pressures
Cells 14B and 15 bonded at 610 → 595°C, 4 minutes, 100 PSI
Cells 7, 13 and 17 bonded at 590 → 575°C, 100 PSI, varied bond time

SECTION IV

CONCLUSIONS

Microprocessor controlled equipment has been used for electrostatic bonding of satellite solar cells to glass covers under controlled environment. Nonreactive environments have resulted in the elimination of cell degradation due to contact corrosion during bonding. New alignment fixturing has been developed to hold the glass and cell during bonding, allowing relaxed tolerances in both glass and cell dimensions.

High-quality electrostatic bonds to MLAR coated cells have been demonstrated, using the technique of "deformation bonding" in the controlled-environment bonder at Spire. These bonds are completely stable under the thermal shock of transfer from liquid nitrogen to boiling water. Bonding has also been demonstrated for vertical junction cells and textured silicon, by using longer and more careful bond cycles. The complete bonding of these materials has not yet been accomplished.

A baseline MLAR coated ESB cell has been defined. This is an OCLI 1-3 ohm-cm cell (lot 8 type). The specifications for this cell are given in Appendix A. Bonds to this type of cell have been demonstrated with 62-64 mW postbond power. Bonds to similar cells, with closer spaced grid lines (lot 83) have been demonstrated with postbond powers of 68 mW. Bonds to MLAR cells made from 10 ohm-cm material have also yielded 62-64 mW bonded cells. Bonds resulting in minimum degradation by use of two-temperature bonding cycles have been identified.

The degradation of cells during bonding has been determined to be due to two causes: pure thermal degradation and voltage-dependent degradation. Some of the pure thermal degradation occurs due to the slow cooldown of bonded samples, and can be avoided by using a modified cooling chamber. Optimized bond cycles involving time/temperature/pressure trade-offs also can lower thermal degradation. Voltage-dependent degradation has not yet been studied in depth.

Deformation bonding has been demonstrated to cells with metallization thicknesses of up to 6 micrometers, twice that specified in the previous study, and line densities of up to 14 lines/cm.

Extended values of time, temperature, and pressure are needed to make deformation bonds to cells with metallization either higher than 3 micrometers or extremely closely spaced. This results in added thermal degradation. There may be an

optimum size and spacing for grid lines for maximum postbond power. Use of cells with aligned "mesa" metallization also seems to have a beneficial effect on postbond power.

Among the highlights of this program to date are:

- Identification of a reproducible MLAR coated solar cell structure that can be electrostatically bonded with 12.5 percent postbond efficiency.
- Elimination of contact adhesion problems by use of total environmental control. Interconnection ribbons, welded to bonded cells, exhibit excellent pull strengths.
- Cell/glass alignment fixturing has been improved significantly, resulting in reduced complexity of the fixture, greater versatility and a relaxation of cell and glass dimensional tolerances.
- Demonstration that deformation bonding offers significant process simplification over use of grooved covers. These improvements include elimination of concerns about stray metallization on the cell surface, elimination of cover grooving, broadening of metallization patterns that can be bonded (e.g., violet cell, chevrons, and all other nonrectangular designs), and a resulting structure that is truly integral.
- Parametric studies have resulted in an improved understanding of the interrelationship of process variables, yielding considerable improvement of bond cycles.
- Thermal degradation rates have been established for some cell types.
- Confirmation of the improved thermal tolerance observed for cells with metallization fabricated in a mesa structure.
- Identification of MoAg as a metallization with significant potential for a high temperature contact.
- Preliminary results on vertical junction cells that indicate that not only is electrostatic bonding a feasible method of covering these cells but also that it may be the most effective way of eliminating the cell breakage problems associated with conventional glued covers.

Problem areas identified in the initial phase of this program include:

- Yield of bonded assemblies with high electrical performances has been lower than desired.
- The present electrostatic bonding facility, while offering significant advantages and improvements over earlier equipment, was constructed for the purpose of bonding relatively large area samples (to 8" x 8") and is thus not ideally suited to 2 x 2 cm structures. This factor alone has contributed significantly to yield problems.
- Although cell specification tolerances have been relaxed due to some of the program developments, the broadened limits must be met if yield of high output bonded assemblies is to reach acceptable levels.
- Discrepancies between measurements at different facilities can result in uncertainties in cell efficiencies of as much as 0.5 percent.
- The method in which bonding voltage is applied may affect cell degradation.

APPENDIX A

ESB SOLAR CELL SPECIFICATION SHEET

BASELINE CELLS

1.0 MATERIALS

1.1 Silicon
- 1.1.1 Type: N/P
- 1.1.2 Resistivity: 2 ohm-cm

1.2 Contact Metallization
- 1.2.1 Front: TiAg
- 1.2.2 Back: TiPdAg

1.3 Coatings
- 1.3.1 Antireflective Coating: MLAR

2.0 CONFIGURATION

2.1 Dimensions (inches)
- 2.1.1 Lateral: 0.790" x 0.790" + 0.002", all dimensions
- 2.1.2 Thickness: 0.010" $\pm$ 0.001"

2.2 Surface Finish
- 2.2.1 Front: Chem/Mechanical Polish
- 2.2.2 Back: Etched

2.3 Surface Preparation
- 2.3.1 Flatness: 200 nm RMS

2.4 Contact Pattern
- 2.4.1 Lines/cm: 12.5
- 2.4.2 Height: 3 μm
- 2.4.3 Ohmic Bar: 0.020" wide

3.0 PERFORMANCE

3.1 Electrical
- 3.1.1 P_{max}: 62 mW minimum

3.2 Thermal
- 3.2.1 Thermal Stability: 570°C - 10 minutes in N_2 degrade less than 5 percent and P_{max} not less than 62 mW

APPENDIX B

ESB SOLAR CELL SPECIFICATION SHEET:

MLAR CELLS

1.0 MATERIALS

1.1 Silicon
- 1.1.1 Type: N/P
- 1.1.2 Resistivity: 2 ohm-cm

1.2 Contact Metallization
- 1.2.1 Front: TiPdAg
- 1.2.2 Back: TiPdAg

1.3 Coatings
- 1.3.1 Antireflective Coating: MLAR

2.0 CONFIGURATION

2.1 Dimensions (inches)
- 2.1.1 Lateral: 0.790" x 0.790" + 0.002", all dimensions
- 2.1.2 Thickness: 0.010" $\pm$ 0.001"

2.2 Surface Finish
- 2.2.1 Front: Chemical Polish
- 2.2.2 Back: Chemical Polish

2.3 Surface Preparation
- 2.3.1 Flatness: 500 nm RMS

2.4 Contact Pattern
- 2.4.1 Lines/cm: 6
- 2.4.2 Height: 3 μm maximum; no cross lines
- 2.4.3 Ohmic Bar: 0.020" - 0.30" wide

3.0 PERFORMANCE

3.1 Electrical
- 3.1.1 P_{max}: 62 mw minimum

3.2 Thermal
- 3.2.1 Thermal Stability: 570°C - 10 minutes in N_2 degrade less than 5 percent and P_{max} not less than 62 mW

APPENDIX B (Concluded)

ESB SOLAR CELL SPECIFICATION SHEET:

MLAR CELLS WITH BACK SURFACE FIELD (BSF)

1.0 MATERIALS

1.1 Silicon
- 1.1.1 Type: N/P
- 1.1.2 Resistivity: 10 ohm-cm

1.2 Contact Metallization
- 1.2.1 Front: TiPdAg
- 1.2.2 Back: TiPdAg

1.3 Coatings
- 1.3.1 Antireflective Coating: MLAR

2.0 CONFIGURATION

2.1 Dimensions (inches)
- 2.1.1 Lateral: 0.790" x 0.790" + 0.002", all dimensions
- 2.1.2 Thickness: 0.010" $\pm$ 0.001"

2.2 Surface Finish
- 2.2.1 Front: Chemical Polish
- 2.2.2 Back: Chemical Polish

2.3 Surface Preparation
- 2.3.1 Flatness: 500 nm RMS

2.4 Contact Pattern
- 2.4.1 Lines/cm: 12.5
- 2.4.2 Height: 3 μm maximum; no cross lines
- 2.4.3 Ohmic Bar: 0.020" - 0.30" wide

3.0 PERFORMANCE

3.1 Electrical
- 3.1.1 P_{max}: 76 mw minimum

3.2 Thermal
- 3.2.1 Thermal Stability: 570°C - 10 minutes in N_2 degrade less than 10 percent

APPENDIX C

THERMAL DEGRADATION TESTS, OCLI LOT 2092

PREBOND MEASUREMENTS

Cell #	V_{oc}(mV)	I_{sc}(mA)	P_{max}(mW)	CFF (%)
16	550	143	55.0	70.0
17	535	141	50.0	66.0
18	535	141	54.0	72.0
21	545	139	52.0	68.0
22	540	144	48.4	62.2
24	530	139	50.0	67.0
26	528	143	56.0	69.0
27	539	141	52.0	68.6
28	537	139	46.0	61.8
31	545	140	51.0	67.0
32	544	143	52.0	66.9
33	550	142	63.0	68.0
34	549	145	57.0	72.0
35	541	143	52.0	67.0
36	542	142	55.0	72.0
45	538	141	52.9	69.7
46	548	140	55.0	71.6
47	545	144	51.7	66.1
57	530	142	50.8	67.6
59	544	142	55.9	72.3
63	530	141	41.0	55.4
64	645	140	53.4	70.0
65	536	143	52.9	69.0
66	505	144	49.1	67.6
66	543	140	53.3	70.2
67	536	138	54.0	73.0
68	547	140	54.5	71.3
69	550	143	57.4	73.3
72	538	142	49.7	70.4
76	538	143	49.5	65.0
77	525	139	52.4	71.9
80	540	142	52.4	68.4
81	546	142	56.3	74.3
83	538	141	51.7	68.1
84	548	138	54.2	72.1
86	524	142	47.7	64.3
88	543	143	56.2	73.6
89	540	140	48.3	63.9
91	541	140	54.2	71.5
92	543	140	55.0	72.9

APPENDIX C (Continued)

THERMAL DEGRADATION TESTS, OCLI LOT 2092

BONDING RESULTS, 570°C TESTS

Bond Duration (min)	Cell #	Percent Change from Prebond Measurement V_{oc}	I_{sc}	P_{max}	CFF
4 1/2 Contact Pressure Only	16	-0.2	-0.2	-1.3	-0.6
	17	+0.4	+0.9	+6.0	+7.0
	18	-0.1	-0.5	-1.9	-2.9
	Avg.	0	+0.1	+0.9	+1.2
4 1/2	21	-1.3	0	+0.6	+4.0
	22	-3.1	-1.0	+8.5	+14.5
	24	-3.0	0	-3.3	-0.6
	Avg.	-2.4	-0.3	+1.9	+6.0
5	26	-3.2	-0.3%	+11.0	+16.0
	27	+0.2	+1.1	+1.9	-0.2
	28	-1.6	+3.2	+13.0	+13.3
	Avg.	-1.5	+1.3	+8.6	+9.7
5 1/2	31	-1.2	+2.1	-4.0	+6.0
	32	+0.1	0	+3.5	+3.0
	33	0	+0.7	-5.6	-6.2
	Avg.	-0.4	+0.9	-2.0	-.9
6 1/2	34	+0.9	-0.7	-1.5	-1.9
	35	+0.7	+0.7	+6.7	+6.0
	36	-0.7	0	+0.2	-5.5
	Avg.	+0.3	0	+1.8	-0.5
8	45	+1.9	+0.7	+2.5	-0.1
	46	0	+2.1	+0.7	-1.4
	47	-0.9	+2.8	+7.9	+5.1
	Avg.	+0.3	+1.9	+3.7	+1.2
10	57	+1.3	-1.8	-4.7	-4.5
	59	0	+0.7	-0.8	-8.7
	63	-3.7	+3.0	+4.9	+6.0
	Avg.	-0.8	-0.6	-0.2	-2.4
15	64	-0.6	+3.6	+1.5	-1.6
	65	-1.9	+1.4	-4.5	-4.1
	66	+5.6	-2.1	-7.3	-10.2
	Avg.	+1.0	+1.0	-3.4	-4.2

APPENDIX C (Concluded)

THERMAL DEGRADATION TESTS, OCLI LOT 2092

BONDING RESULTS, 590°C TESTS

Bond Duration (min)	Cell #	Percent Change from Prebond Measurement V_{oc}	I_{sc}	P_{max}	CFF
4 1/2	68	-1.10	-2.14	-4.25	-0.70
	69	-1.09	-3.50	-6.16	-2.32
	72	-1.12	0	+8.11	+7.15
	Avg.	-1.10±0.02	-1.88±1.76	-0.77±7.75	+1.37±5.07
6	76	-1.48	-0.69	+4.00	+8.15
	77*	0*	-26.6*	-26.9*	0*
	80*	0.55*	-42.9*	-40.3*	+5.26*
	91	0	+2.14	+1.85	-0.56
	Avg.	-0.74±1.05	+0.73±2.00	+2.93±1.52	+3.80±6.16
8	81	+0.73	+1.40	+1.75	-3.63
	83	-2.97	-0.71	-3.92	-1.17
	89	-3.15	-12.1	-12.6	+2.72
	Avg.	-1.80±2.19	-3.80±7.26	-4.92±7.22	-0.69±3.20
10	84	-0.73	-0.72	-4.56	-3.88
	86	-4.20	-7.04	10.6	+2.49
	88	+1.28	-9.09	-29.8	-23.2
	Avg.	-1.22±2.77	-5.62±4.36	-14.9±13.2	-7.27±14.2

Cells 77 and 80 cracked; data from these cells not included in average.

REFERENCES

1. Wallis, G., "Direct Current Polarization During Field-Assisted Glass-Metal Sealing", Journal of the American Ceramic Society, Volume 53, p. 563 (1970).

2. "Stress Free Application of Glass Covers for Radiation Hardened Solar Cells and Arrays", AFAPL Contract F33615-74-C-2001, Interim Report No. AFAPL-TR-75, Simulation Physics, Inc. (now Spire Corp.) (1975).

3. "Stress Free Application of Glass Covers for Radiation Hardened Solar Cells and Arrays", AFAPL Contract F33615-74-C-2001, Final Report No. AFAPL-TR-77-28, Simulation Physics, Inc. (1977).

4. Walker, D.H., Statler, R.L., and Lambert, R.J., "Solar Cell Experiments on the NTS-2 Satellite", Thirteenth IEEE Photovoltaic Specialists Conference, p. 100 (1978).

5. Tada, H.Y., and Carter, J.R., Solar Cell Radiation Handbook, JPL Publication No. 77-56, pp. 6-17 (1977).

6. "Integral Glass Encapsulation for Solar Arrays", DOE/JPL Contract 954521, Interim Report No. 1, Spire Corp. (1977).

7. Faith, T.J., and Iles, P.A., "High Temperature Contacts for Silicon Solar Cells", Thirteenth IEEE Photovoltaic Specialists Conference, p. 321 (1978).

8. "High Efficiency Solar Panel", AFAPL Contract F33615-75-C-2028, Final Report No. AFAPL-TR-77-36, pp. 43-52, Spectrolab (1977).

9. "Non-Reflective Vertical Junction Solar Cells", AFAPL Contract F33615-76-C-2058, Interim Report No. AFAPL-TR-77-38, Solarex (1977).

*U.S.Government Printing Office: 1979 — 657-002/630